STRIDE-TO-STRIDE LOWER LIMB SAGITTAL-PLANE JOINT ANGLE VARIABILITY OF WALKING ACROSS INCLINATIONS

Faculty of Sport and Health Sciences

Chuan-Chih Chiang

Master`s Thesis in Biomechanics
Faculty of Sport and Health Sciences
University of Jyväskylä
Spring 2024
Supervisors: Janne Avela, Neil Cronin, Sailee Sansgiri

ABSTRACT

Chiang, C. 2024. Stride-to-stride lower limb sagittal-plane joint angle variability of walking across inclinations. Faculty of Sport and Health Sciences, University of Jyväskylä, Master's Thesis in Biomechanics, 64 p, 4 appendices.

As walking serves as an indicator of multiple health conditions and quality of life, it is important to obtain a thorough understanding of walking, specifically, gait. When walking in the community, it is inevitable to walk on uneven surfaces, including slopes. The sloped walking is more imbalanced compared to level walking and several alterations in biomechanics are required to adapt to its perturbations. Since the trunk and pelvis manage their position according to the earth's vertical during sloped walking, the lower limbs have to interact with this postural adjustment, leading to changes in kinematics. During walking, the sensorimotor system constantly tunes the movement patterns, and the variance exists from stride to stride. The variability within movement has been found to have a deterministic origin, and it alters when encounters perturbations or new tasks. An increased variability has been correlated to decreased balance performance or enhanced adaptability of movement strategy. Extremely high or low variability is considered an impairment or unhealthy condition. So far, there haven't been many studies about gait variability during sloped walking and more studies are mandatory to reveal how sensorimotor strategy alters. As a result, this study aims to investigate the stride-to-stride lower limb sagittal-plane joint angle variability during uphill and downhill walking.

The participants were healthy adults (Age: 34.2±7.6, 13 females). They were asked to walk on the treadmill at a constant self-selected speed and at 0°, ±2°, ±4°, ±6°, and ±12° inclinations. Motion data was collected by an 8-camera motion capture system with a sampling rate of 200 Hz. Plug-in-Gait lower body model was applied for kinematic analysis. Thirty participants' data were included in the analysis. An automatic gait event detection based on marker displacement was adopted to estimate the gait events. The sagittal-plane joint angle variability was calculated through a linear method, mean standard deviation, and a non-linear method, sample entropy.

The results showed that the inclinations had significant effects on the spatiotemporal parameters and the lower limb sagittal-plane joint angle variability. The alterations in the spatiotemporal parameters indicated that the participants favored a more conservative gait during downhill and steep uphill walking. Stride-to-stride sagittal-plane joint angle variability generally increased as the inclinations increased. Specifically, the amount and the structure of the sagittal-plane joint angle variability increased during downhill walking compared to level walking. On the other hand, during uphill walking, the amount of the sagittal-plane joint angle variability incrementally increased as the inclination increased, while the structure of the sagittal-plane joint angle variability decreased at lower inclines and increased at the highest inclines. Overall, the results indicated that the healthy adults used a more flexible movement strategy during sloped walking. The alteration in the sagittal-plane joint angle variability suggested that the sensorimotor strategy was task-specific, and it might change in response to the balance perturbations, muscular coordination, and power demands during walking on inclined surfaces.

Keywords: variability, joint angle, slope, walking, gait

ABBREVIATIONS

ANOVA	analysis of variance
ApEn	approximate entropy
COG	center of gravity
COM	center of mass
CKC	closed kinematic chain
FS	foot strike
FO	foot off
MoCap	motion-capture
OKC	open kinematic chain
SampEn	sample entropy

CONTENTS

1 INTRODUCTION

Walking is one of the most important functions in our daily life. Scientific and clinical fields have adopted the ability to walk as an indicator of the coordination of movement, the progress of rehabilitation, the risk of medical conditions, the functional fitness level, the risk of falling for the elderly or population with movement disorders, and the quality of life (Lee et al. 2021). When walking in the community, we encounter obstacles, turns, stairs, slopes, and different surfaces. Thus, studying walking in various conditions is important to understand it thoroughly.

During sloped walking, movement is altered to fulfill the different requirements of foot clearance and foot placement and is carried out by a serial adjustment of the body segments and postural support (Prentice et al. 2004). Especially on higher inclinations, the biomechanics of gait considerably differ from the level ground walking (Kawamura et al. 1991). The major tasks of uphill walking are propelling the center of mass upward and forward (Leroux et al. 2002) and making sufficient foot clearance and longer strides during the swing phase (Leroux et al. 2002; McIntosh et al. 2006; Wen et al. 2019). In contrast, downhill walking draws attention to energy absorption and impact management (Leroux et al. 2002; McIntosh et al. 2006). Walking downhill is also challenging to maintain balance and requires more energy consumption to recover from perturbations (Dewolf et al. 2020).

When we walk, none of the movement patterns in our strides are exactly repeated (Newell and Corcos. 1993). This variance within the repetitive movement task has been explained by a concept called movement variability (Stergiou. 2004). Movement variability was once thought to be a random error or noise (Harris and Wolpert. 1998). However, recent studies found it to be deterministic (Hausdorff et al. 1996) and serve a functional role in the sensorimotor system (Hamill et al. 1999). To be more specific, the variability allows the sensorimotor system to be more flexible and adaptive to perturbations or yields a chance to try and learn a new movement pattern (Stergiou. 2004). For example, several articles have presented that joint angle variability increases in response to perturbations, such as unstable surfaces (Mohr et al. 2023) and higher impacts on the limb (Estep et al. 2018). A similar phenomenon was also observed during sloped walking, in which movement variability increased when the inclination of the walking path increased (Dewolf et al. 2020; Sarvestan et al. 2021).

When using linear mathematics to examine movement variability, the outcome shows the amount of variability (Harbourne and Stergiou. 2009). A non-linear method is more suitable to examine the complexity of movement and it reveals the structure of variability (Stergiou. 2004; Harbourne and Stergiou. 2009). So far, no studies have examined stride-to-stride joint angle variability in downhill walking, nor has research been conducted with a non-linear method. Therefore, to better understand how the sensorimotor system reacts to inclinations, the present study investigated stride-to-stride lower limb sagittal-plane joint angle variability during walking across inclinations, including uphill and downhill, with a linear and a non-linear method.

2 ANATOMY OF LOWER LIMBS

The human body can be categorized into three major components: upper extremity, trunk, and lower extremity. The lower extremity yields most of the movement during human ambulation, which makes it important to understand the structures comprised of it. Thus, this chapter will focus on the anatomy of the lower extremities, including the terminology describing movements.

2.1 Terminology

Kinematics is a term for mechanics of the motion of a body (Neumann. 2017). There are a few aspects for describing the motion in Kinematics, including planes of motion, axis of rotation, and degrees of freedom. When a human is standing in an anatomical position (Figure 1), the sagittal plane is the one that runs in between the body's left and right sides; the frontal plane separates the body into back and front parts, and it faces the same direction where the body's facing; the horizontal or the transverse plane divides the body into upper and lower parts, which is parallel to the standing surface (Neumann. 2017). The axes of rotation are perpendicular to the planes of motion. The one perpendicular to the sagittal plane runs in the direction of the mediolateral; for the frontal plane, the axis is in an anterioposterior direction; the axis for rotating on the horizontal plane is referred to as the superioinferior or vertical axis (Neumann. 2017). Regarding the relative position, the term proximal represents being closer to the center of the human body, and distal is referred to the opposite direction.

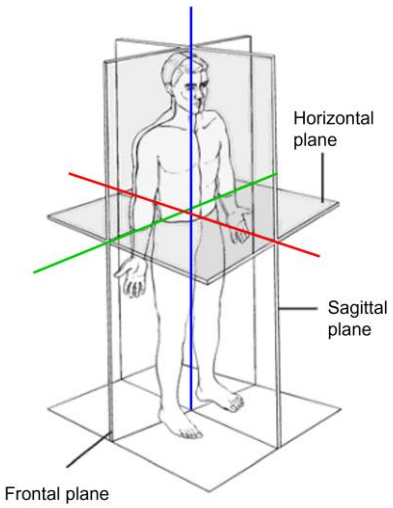

FIGURE 1. Planes of motion and axes of rotation. Adapted and revised from Anang et al. (2016).

Generally, the motions on the sagittal plane that go forward and backward of the anatomical position are defined as flexion and extension respectively; on the frontal plane, the motion moving away from the body's mid-line is referred to as abduction, and the motion is the reverse is adduction; the motions on the horizontal plane are internal rotation and external rotation, defined by the direction of body segments rotating toward (Calais-Germain. 2007). However, the terms for motion may differ according to the body segments. For example, the motions of the ankle joint are defined as plantar flexion and dorsiflexion on the sagittal plane.

The degree of freedom is defined as the number of independent directions of movement allowed at a joint, as well as the number of permitted planes of angular motion (Neumann. 2017). For example, if a joint allows motions on three planes, it has three degrees of freedom.

The open kinematic chain (OKC) refers to the condition that the distal segment moves freely in the space, and the movement results from the distal segment rotating on the proximal segment. In contrast, the closed kinematic chain (CKC) describes that the distal segment is fixed in an immovable object, e.g. earth, and therefore the proximal segment becomes the one rotating on the distal segment (Neumann. 2017).

2.2 Bones and joints

The following paragraphs focus on the interested joints in this study, which are the hip, knee, and ankle joints, and the bones consist of the joints. The joint is formed as the neighboring bones are linked, and the joints dominant in lower limb movements are synovial joints (Calais-Germain. 2007). Depending on the linking spot of bones, which is the articular surface, the synovial joints in lower limbs can be further categorized into ball-and-socket, hinge, ellipsoid, plane, and condyloid joints (Neumann. 2017).

2.2.1 The hip joint

The pelvis consists of ilium, pubis, and ischium bones of both the left and right side, which is a bowl-shaped segment connecting the trunk and lower limb. The pelvis serves an important role in the common attachment of muscles in the lower limb (Neumann. 2017). The femur is the bone of the thigh segment, whose structure can be subdivided into the head, neck, and shaft.

The hip joint, a general term for the coxofemural joint, is formed with the acetabulum of the pelvis and the femoral head. As a ball-and-socket joint, the hip allows more degrees of freedom in motion (Calais-Germain. 2007). Since joint stability is determined by both articular geometry and soft tissue integrity (Fetto. 2019), the hip joint, surrounded by strong muscular and ligamentous structures, provides essential stability during walking (Calais-Germain. 2007; Neumann. 2017).

The hip performs flexion, extension, abduction, adduction, external rotation, and internal rotation from the aspect of femur-on-pelvis rotation. The terms for motions of pelvis-on-femur rotation are mostly the same, except that they refer to anterior and posterior pelvic tilt on the sagittal plane (Neumann. 2017).

2.2.2 The knee joint

The tibia and fibula are located below the femur, and they run parallel to each other. While only the tibia makes contact with the distal femur, the fibula assists in transferring the load between the knee and ankle (Neumann. 2017). The patella is a sesamoid bone, indicating that it is embedded in the tendon. The quadriceps femoris tendon runs over the patella, extends inferiorly, and inserts at the tibial tuberosity (Neumann. 2017).

The knee joint is a general term, which combines two joints: the femoropatellar joint and the femerotibial joint. The knee is recognized as a condyloid joint (Neumann. 2017) or a hinge joint (Calais-Germain. 2007) since its motions occur majorly on the sagittal plane. The motions of the femorotibial joint on the frontal and the horizontal plane are restricted by the surrounding ligaments, including medial collateral, lateral collateral, anterior cruciate, and posterior cruciate ligaments (Calais-Germain. 2007).

Aside from the independent motion on the sagittal and horizontal planes, the knee extension is accompanied by external rotation at the last 30 degrees, which is described as the screw-home mechanism. The screw-home mechanism ensures the maximum contact area between the femur and tibia, and therefore, supports the knee joint stability at extension (Neumann. 2017).

2.2.3 The ankle and foot joint

The ankle and foot contain 27 bones, and the latter can be subcategorized into rearfoot, midfoot, and forefoot.

The ankle joint is a collective term that includes multiple articulations of the tibia, fibula, and talus. Since the tibia and fibula bones contact each other at both proximal and distal ends, they form a tibiofibular joint at these two spots. Furthermore, the concavity forming by the distal end of the tibia and fibula is further adjacent to the talus bone, forming the talocrural joint. Due to the bony structure and strong soft issues surrounding the talocrural joint, it allows mostly plantar flexion and dorsiflexion, while limiting the motions rotating on other axes (Calais-Germain. 2007; Neumann. 2017).

The subtalar joint comprises the talus and calcaneus, providing motions on the three axes. Unlike the definition for the joints mentioned above, the subtalar motions rotating at the anterioposterior axis are defined as eversion and inversion, and at the superioinferior axis, they are referred to as abduction and adduction (Neumann. 2017). Moreover, the subtalar joint allows little plantar flexion and dorsiflexion. In addition to the three ordinary motion axes, the subtalar joint has a fourth axis called the axis of Henke, which runs anterosuperomedially, introducing the combined motions: pronation and supination (Calais-Germain. 2007; Neumann. 2017). Pronation is a combination of plantar flexion, inversion, and adduction. On the other hand, supination consists of dorsiflexion, eversion, and abduction (Calais-Germain. 2007; Neumann. 2017).

The transverse tarsal and distal intertarsal joints in the midfoot, as well as the joints in the forefoot, present important functions during locomotion (Fraser et al. 2016). Previous literature concluded that footwear restricts foot motion in sagittal, frontal, and horizontal planes and the changes in medial longitudinal foot arch (Franklin et al. 2015). While the participants in the present study wore shoes during walking, the motion of the midfoot and forefoot may be minimized. Furthermore, the adopted model for further analysis does not segment the ankle and foot. Thus, they will not be further discussed in this chapter.

3 GAIT

Walking is a method of locomotion, normally including support and propulsion, while gait is a term for describing the manner or style of walking (Whittle. 2007). The gait may be affected by many factors, including age, body weight, and pathology, and it is also associated with quality of life (Lee et al. 2021). As a result, it is important to understand the fundamentals of gait. This chapter introduces the terminology in gait analysis, the normal gait, and the gait on inclined surfaces.

3.1 Gait cycle and spatiotemporal parameters

A gait cycle during normal walking consists of two major phases, the stance phase, and the swing phase. Stance phase describes the period when the foot has contact with the ground. On the other hand, the swing phase refers to the time when the foot is moving through the air. Some specific time points when one lower limb interacts with the walking surface or the opposite limb are defined as gait events. They are used to further subdivide a gait cycle into loading response, mid stance, terminal stance, pre-swing, initial swing, mid swing, and terminal swing by major gait events (Whittle. 2007). A gait cycle can start from any of the major gait events and end at the same event which happens successively.

Most studies in gait analysis mark the time point when the foot first touches the ground, which is initial contact, as the starting point of a gait cycle (Figure 2). The sequence of gait events following the initial contact is opposite toe off, heel raise, opposite initial contact, toe off, free adjacent, and tibia vertical. Toe off describes the last moment when the foot contacts the ground, and it also represents the beginning of the swing phase. The double support phase is defined as the period between the initial contact and the opposite toe off. Before the opposite initial contact happens, the time only one leg is on the ground is called the single support phase. (Whittle. 2007)

According to Whittle (2007), the general portion of the stance phase, swing phase, and double support phase is 60%, 40%, and 10% respectively. Nevertheless, the duration of each phase is also affected by the walking speed: generally, with increased walking speed, the swing phase is lengthened, and the stance phase is shortened (Tulchin et al. 2009; Hebenstreit et al. 2015; Núñez-Trull et al. 2023).

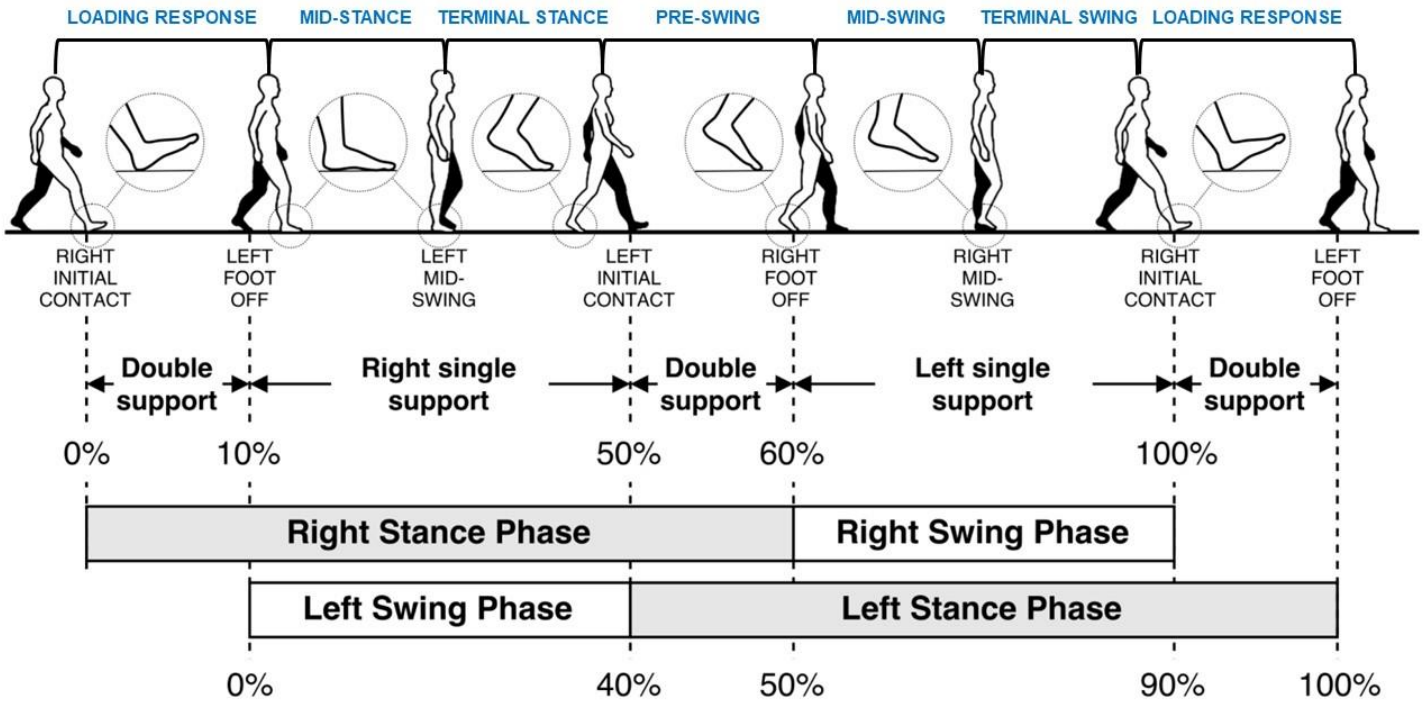

FIGURE 2. The major events and phases of a gait cycle. Adapted and revised from Tunca et al. (2017).

The terminology of gait events varies among studies since the movement pattern may differ from normal and pathological gaits. For example, one alternative for the initial contact is the heel strike. However, in populations with spastic cerebral palsy, the initial contact is not always made with the heel but with the forefoot (Bauer et al. 2022). According to the previous research (Alexander and Schwameder. 2023), 88.9% of the subjects sustained a heel strike pattern during 12° uphill walking. Considering the potential variant patterns during hill walking, it would be more suitable for this study to adopt the foot-strike (FS) as initial contact and foot-off (FO) as toe off.

The spatiotemporal parameters regarding the foot placement include stride length, step length, and step width. Stride length describes the distance between two consecutive placements of the same foot, and one stride consists of two steps (Whittle. 2007). Step width measures the distance between two heels in a mediolateral direction, which has been associated with balance control (Stimpson et al. 2019). The time interval between two successive strides represents the stride time, which is also the duration of a gait cycle. The term for the number of steps per minute is

cadence. In overground walking, the walking speed is the quotient of stride length and stride time. For the healthy adult population, the spatiotemporal parameters mentioned above were not only frequently measured in the previous studies, but also are the most relevant biomechanical parameters in gait analysis (Roberts et al. 2017).

3.2 Kinematics of gait

During walking, the movements occur mostly on the sagittal plane. Starting from the hip movement at initial contact, it begins to extend from a flexed position and later turns into an extended position during mid-stance. After the peak hip extension (10°-20°) occurs at around the opposite foot-strike, the direction of the movement reverses into flexion, which happens before the foot-off. The maximum hip flexion (around 30°) is reached in mid-swing and maintained until the next foot-strike. (Whittle. 2007)

The knee is almost fully extended at the foot-strike. It begins to flex during loading response and reaches the first flexion peak (10°-20°) early in mid-stance. Then the movement of the knee reverses into extension until peak knee extension at heel rise. As the gastrocnemius activates for propulsion, the knee flexion is initiated again and reaches its maximum flexion (60°-70°) during the initial swing. During this phase, the movement is majorly carried out by the flexing hip, which is also called the double pendulum. Due to the same effect, the knee has started to passively extend before the feet are adjacent. (Whittle. 2007)

The ankle is approximately neutral, and the foot is slightly supinated at the foot strike. The ankle dorsiflexors eccentrically lower down the foot to plantar flexion during the first half of the loading response and reverse to concentric contraction during the second half. Meanwhile, the foot begins to pronate with an internally rotating tibia. They reverse the motion soon after reaching the peaks around the opposite foot-off. The peak dorsiflexion happens during the terminal stance and starts to plantarflex afterward. While the heel has already lifted off the ground, the toe is still flat on it. The foot later reaches the peak supination with hindfoot inversion and coupled tibia external rotation. When combined with the stretch of the plantar fascia, the foot is highly stable. The peak ankle plantar flexion (around 25°) appears after the foot-off. (Whittle. 2007) During the swing phase, it is important for the ankle to stay neutral or dorsiflexed to complete the foot clearance, thus avoiding tripping (Pijnappels et al. 2001; Rosenblatt et al. 2014a).

3.3 Effect of inclination on gait

Commonly, people encounter surfaces with different inclinations when walking in communities. An increased risk of falling on inclined surfaces (Sheehan and Gottschall. 2012) makes it important to understand the biomechanics of sloped walking. Humans adapt to sloped surfaces through changes in kinematics and kinetics (Zeng et al. 2022). Generally, modifications occur in foot clearance and placement, movements of body segments, and postural support (Prentice et al. 2004). The primary postural adjustment for sloped walking is achieved by altering the orientation of the trunk and pelvis relative to the earth's vertical in sagittal plane while maintaining the same movement across different inclinations and is task-specific (Leroux et al. 2002). Furthermore, the pelvis interacts with the lower limbs to smoothen the trajectory of the center of gravity by reducing its displacement (Leroux et al. 2002). The critical inclination leading to changes in the center of pressure falls between 9 to 12 degrees (Kawamura et al. 1991).

3.3.1 Spatiotemporal parameters of sloped walking

When humans walk at a self-selected speed across inclinations, they tend to decrease their walking speed as a result of decreased cadence at uphill conditions and decreased step length at downhill conditions (Kawamura et al. 1991). The later studies observed similar changes in spatiotemporal parameters in sloped walking as the speed remained the same: the cadence decreased with increasing inclination in the positive direction, and it increased with increasing inclination in the negative direction (Leroux et al. 2002; McIntosh et al. 2006). Leroux et al. (2002) stated that the decreased cadence, which implied increased stride length as the walking speed remained the same, was associated with generating greater momentum for walking on steeper uphill surfaces. The major tasks during downhill walking are braking and balancing the center of gravity, and the shortened step length assists in stabilizing the knee and ankle joints (Kawamura et al. 1991). Similarly, Dewolf et al. (2020) suggested that the increased step width on slopes and shortened stride length on negative slopes were movement strategies to maintain gait stability, and further specified that people used a more cautious gait pattern during downhill walking. This behavior was also observed by other researchers. For example, Bueno et al. (2019) reported a significantly shortened stride length during walking with increased fear of falling on older females.

3.3.2 Kinematics of uphill walking

As the body is passively pulled backward by gravity during uphill conditions, the trunk and pelvis actively forward tilt to counteract this effect. This forward-leaning posture moves the center of gravity ahead of the base of support and assists in propelling movement (Leroux et al. 2002). Generally, the amount of lower limb joint flexion increases linearly with increased inclination (Hong et al. 2014). McIntosh et al. (2006) reported that the hip flexion angle at heel strike and knee flexion angle in early stance increased during uphill walking. Zeng et al. (2022) reported significant differences in knee sagittal, frontal, and horizontal joint angles when comparing 15% uphill walking to level walking. Additionally, an increase in anterior tibial translation was observed during uphill walking. Wen et al. (2019) concluded that, as inclination increased, knee extension ROM increased while knee flexion ROM decreased, reflecting adaptations for lifting the body on inclined surfaces. The increased ankle dorsiflexion angle in the first half of the gait cycle and the increased ankle plantar flexion at toe off were observed during uphill walking (McIntosh et al. 2006; Sarvestan et al. 2021). The behavior of the ankle is altered to adapt to the change in the trunk and pelvis orientation (Leroux et al. 2002), which indicates a large demand for ankle ROM during uphill walking (McIntosh et al. 2006). The lower limb movement patterns at a higher positive inclination (10°) differ from the ones at the level ground in the sagittal, frontal, and horizontal planes, while the patterns at a lower positive inclination (5°) show clear differences only in the sagittal plane (Sarvestan et al. 2021).

The increased hip flexion and knee flexion during the swing phase account for overcoming the inclined surface and generating greater stride length (Leroux et al. 2002; McIntosh et al. 2006; Wen et al. 2019). Meanwhile, the lateral pelvis tilt toward the swinging leg decreases, which allows the greater lift of the swinging leg (Leroux et al. 2002).

3.3.3 Kinematics of downhill walking

During downhill walking, the body is passively pulled forward and downward by gravity, so the trunk and pelvis perform backward tilting to move the center of gravity backward (Leroux et al 2002). McIntosh et al. (2006) presented that the hip flexion angle at the heel strike decreased during downhill walking. While there is no difference in the knee angle at the heel strike between the level ground and downhill walking, the minimum knee flexion angle in the

stance phase increases (McIntosh et al. 2006). The ankle plantarflexion decreases as the surface becomes steeper (McIntosh et al. 2006). The knee of the support limb plays an important role in lowering the body during downhill (Redfern and DiPasquale. 1997). Nevertheless, the task of power absorption is performed mainly by the hip and ankle (McIntosh et al. 2006).

Regarding the kinematics of the swinging limb, the lateral pelvis drop increases (Leroux et al. 2002). Moreover, there are decreases in hip flexion and increases in knee flexion of the swinging limb, and the latter could mainly account for the decrease in stride length, vertical displacement of the center of mass, and the impact force at heel contact (Leroux et al. 2002).

The management of movement strategy during downhill was mainly for recovering from perturbations and reducing risks of falls, however, costing higher energy consumption (Dewolf et al. 2020).

4 MOVEMENT VARIABILITY

Movement variability is defined as the normal changes in motor performance across multiple repetitions of a task (Stergiou. 2004). In other words, it's impossible for humans to repeat the same tasks in exactly identical movement patterns (Newell and Corcos. 1993). Traditionally, the variations in movements were interpreted as random fluctuations, which is noise, in the sensorimotor system (Harris and Wolpert. 1998). However, the recent literature revealed that the phenomenon is a result of nonlinear interaction and is distinguishable from the random noise (Hausdorff et al. 1996). Stergiou (2004) summarized the variability model in which the total variability consisted of the variability due to the nonlinear dynamical process and the variability due to errors. The errors were further subcategorized into biological errors within the neuromotor system, errors from the methodological process, and errors due to external sources, such as environments and task requirements (Stergiou. 2004).

4.1 Interpretation of movement variability

Variability in movements was interpreted as a limiting factor in traditional concepts of motor control. To be more specific, the increased variability was thought to be associated with less stability in the sensorimotor system (Boucher et al. 1995; Maki. 1997). The increased kinematic variability at the hip, pelvis, and trunk during walking was observed in people with hip pain, which might indicate a reduced neuromuscular control or a strategy to alleviate pain (Loverro et al. 2019). This point of view was opposed by Dingwell and Cusumano (2000). They highlighted that the concepts of variability and local dynamic stability should be differentiated, and neither of them was the major factor of increased risks of falling in neuropathic patients (Dingwell and Cusumano. 2000).

Hamill et al. (1999) suggested that the variability in movement had a functional role in motor control when investigated with the dynamic system approach. Correspondingly, Stergiou (2004) summarized several benefits of movement variability, including allowing a more flexible neuromotor system to learn new movement patterns through adjusting and rescaling parameters, and an opportunity to select the most appropriate pattern by sampling different movement patterns. For instance, people walking in high heels showed higher ankle joint angle variability than in barefoot to counteract unstable situations (Alkjær et al. 2012). Mohr et al. (2023) reported that the unstable running surface resulted in a higher stride-to-stride variability of

postural changes which might result from the adaptation within each stride to achieve an economical movement pattern. Blair et al. (2018) demonstrated that, regardless of the gait speed, the lower limb kinematic and muscle activity variability increased during walking on the uneven surface. Since the pronounced alterations in variability occurred at initial contact, they assumed that increased variability might be an anticipatory strategy for lower limbs to adapt to the irregular surfaces (Blair et al. 2018). Aside from the impact of surfaces, the unstable movement may affect variability as well. Running, subject to larger forces and impacts, movement at higher speed, and higher demand for coordination, was reported to have higher hip and knee joint angle variability than walking (Estep et al. 2018).

Kweon et al. (2022) observed that people with chronic ankle instability had higher joint coupling angle variability during the stance phase in gait, which indicated a strategy aiming to distribute the load with more flexible movement patterns. To be more specific, the movement variability could alter according to the demands of sensorimotor function in each gait phase (Kweon et al. 2022). Hypothetically, the increase in movement variability may be adopted as one strategy to maintain the stability of the gait pattern in response to perturbations, or to fulfill the precision requirements during constrained walking (Tokuda et al. 2018; Rosenblatt et al. 2014b). However, Treda et al. (2015) showed that, compared to the control group, the participants with chronic ankle instability had a lower frontal plane ankle joint variability as they intended to minimize ankle giving-away (Treda et al. 2015). It revealed that the movement strategy could be altered by chronic instability and the rehabilitation program should be designed to regain adaptability and flexibility in the sensorimotor system (Treda et al. 2015).

On the joint aspect, McCamley et al. (2018), with non-linear analysis, observed that the stride-to-stride joint angle variability was highest at the ankle and lowest at the hip during treadmill walking. Correspondingly, Fallahtafti et al. (2022) reported the highest stride-to-stride joint angle variability at the ankle, but the joint angle variability of the hip was higher than the knee in both pre- and post-exercise intervention in patients with peripheral artery disease.

Even though the optimal range of variability hasn't been defined, previous studies hypothesized that either excessive or insufficient variability was related to an increased risk of falls (Brach et al. 2005) and a higher risk of injury (Hamill et al. 2012; Baida et al. 2018). One systematic review reported that the results of the relationship between movement variability and lower limb injury were inconsistent among studies, and the direction of changing variability may be

in response to movement tasks, pain, or injuries (Baida et al. 2018). Blyton et al. (2023) suggested the alterations in variability in injured runners may be a strategy to compensate for the injury-related symptoms and they were more likely to occur at proximal segments. Both Baida et al. (2018) and Blyton et al. (2023) mentioned the divergence of analysis methods and parameters for examining the movement variability, which led to difficulties in comparing results from different studies and drawing robust conclusions.

4.1.1 Effect of inclinations on movement variability

Dewolf et al. (2020) observed that the thigh elevation angle variability significantly increased at -6 and -9 degrees of sloped walking, the shank elevation angle variability increased on +6 and +9-degree slopes, and the foot elevation angle variability only increased on -9-degree slope. With a similar linear method, Sarvestan et al. (2021) examined the stride-to-stride lower limb joint angle variability at 0-, 5-, and 10-degree uphill walking via a linear method and reported that the ankle joint angle variability decreased in the frontal and horizontal plane while increasing in the sagittal plane as the positive inclination increased; during the stance phase, the knee joint angle variability increased on the sagittal and frontal plane at the higher inclination during stance phase, but decreased on the horizontal plane; although significant differences in the hip joint angle variability were observed on the sagittal and frontal plane, they occurred within a relatively small portion of gait cycles. Generally, the higher hip, knee, and ankle joint angle variability in the sagittal plane implied that the sagittal movement played a major role in responding to perturbations during uphill walking (Sarvestan et al. 2021). Ippersiel et al. (2022) investigated the lower limb kinematic variability when their participants walked on various uneven surfaces. They found that the knee-hip coordination variability on uphill and downhill increased compared to level ground, indicating that sloped walking was a more challenging task for the neuromuscular system (Ippersiel et al. 2022). To date, there hasn’t been a study investigating stride-to-stride joint angle variability during downhill walking, nor has there been one done with the non-linear method. A study that reveals alteration in stride-to-stride joint angle variability involving these elements allows further understanding of the sensorimotor strategy of human walking.

5 METHODOLOGY OF GAIT ANALYSIS

For gait analysis, it is mandatory that the method not only captures the continuous walking motion but also permits investigations at certain time points. One common method to acquire three-dimensional (3-D) kinematic data is through motion-capture (MoCap) systems with optical devices, such as cameras. Without the device for force detection, the gait events are identified by the algorithm which is established solely on kinematic data. The joint angles are normalized to the gait cycle and are further calculated through specific mathematics to quantify the variability. Accordingly, this chapter will introduce how the optical MoCap system records movements and transforms them into biomechanic parameters, the algorithms for detecting gait events, and the mathematics for quantifying movement variability.

5.1 Optical motion capture system

The practice of using optical devices to study gait can be traced back to Muybridge (1887), in which the locomotion in phases of the horse was captured by a high-speed camera. This breakthrough allowed people to study movement at a certain status and repeat inspection without asking the subject to perform it over and over again. Nowadays, researchers build MoCap systems with more than two cameras, enabling them to capture 3-D motion. Some principles of photography between using traditional and modern equipment are similar. For instance, the light of the environment affects the imaging more or less (Robertson et al. 2014), and factors such as sampling frequency determine the detail within the recorded movement (Marmelat et al. 2019; Fallahtafti et al. 2021). Although sampling frequency at 240 Hz is considered as gold standard, previous studies concluded that 120 Hz was enough for gait kinematic analysis (Marmelat et al. 2019; Fallahtafti et al. 2021). The required sampling rate increases as the speed of movement increases.

To correlate the space presented in the 3-D optical MoCap system to the real world, the cameras are calibrated with a real-world reference, usually a calibration wand. After the capture volume of the space is established, the Cartesian coordinate is adopted to describe spatial information. The global coordinate system (GCS), whose X- and Y-axis are parallel to the level ground surface, the Y-axis points anteriorly, and the Z-axis points superiorly, with an origin at (0, 0, 0), tells the capture volume and the location of a specific point in the system (Robertson et al. 2014). Since we are interested in the relative movement of body segments, the local coordinate system

(LCS) is required in the system, which allocates another X, Y, and Z axes for the body segments. Typically, the local coordinate system treats the location of the center of mass (CoM) of the segment in the reference frame as the origin (Robertson et al. 2014). From GCS, we only obtain the displacement of the CoM of the segment in the space, while we acquire how the segment rotates by comparing the LCS axes to the GCS.

When inspecting the images recorded by cameras, we are not able to locate the center of mass of the segment with human eyes. Instead, we track the prominent points on the subject, such as bony landmarks or markers. With a marker-based method, reflective markers are attached to the moving limbs, and the segments are later reconstructed based on the marker setup. In 3-D analysis, it is essential to have at least three noncollinear markers mounted on the target segment for computing the LCS (Robertson et al. 2014). Since the markers are used to represent the segment, the issues associated with the marker placement (e.g. soft tissue artifacts and marker displacement) may negatively influence the validity of the results (Leboeuf et al. 2023). Moreover, the markers are regarded as reference points when estimating joint centers (Kadaba et al. 1990; Nair et al. 2010). It is suggested that the researchers inspect the marker placement on the subject before recording the trial to minimize human error (Robertson et al. 2014).

To investigate the interaction between two body segments, e.g. joint angle, a link-segment model that links the segments to each other with joints is applied and the LCSs of the segments are compared (Robertson et al. 2014). One common assumption among link-segment models is that the segment is rigid and the mass concentrates at its CoM (Kingma et al. 1996), which enhances feasibility in mathematics (Robertson et al. 2014). However, this assumption may fail to simulate the important biological features of some human body segments. For example, in some commonly used rigid ankle-foot models, the hindfoot, midfoot, and forefoot are recognized as one single rigid segment. This simplification overlooks the functionality of the flexible foot which plays an important role in transmitting forces during locomotion (Erdemir et al. 2004; Bruening et al. 2012) and further introduces certain concerns in applying the rigid-foot-segment model in kinematic and kinetic analysis (Pothrat et al. 2015; Dixon et al. 2012). In this case, the link-segment models which define the ankle and foot as multiple segments can provide a more thorough understanding of the foot biomechanics, while it also requires more effort in subject preparation and data analysis. Accordingly, when selecting the link-segment model, researchers should take both the study design and the cost efficiency into consideration.

As mentioned above, the marker-based system requires at least three markers to construct the LCS for a segment. Marker occlusions in the recording movement, which are gaps, may lead to inaccuracy in the results (Camargo et al. 2020; Mohammadzadeh Gonabadi et al. 2022). To reduce the gaps within the data to a minimum, scientists and the MoCap system providers have proposed several gap-filling methods that estimate the marker trajectory by interpolation. For example, the commonly used Vicon Nexus software (Vicon Motion Systems Ltd., Oxford, UK) provides the spline fill, pattern fill, rigid body fill, and kinematic fill functions, potentially saving time and effort in data processing (Camargo et al. 2020). To be more specific, the spline fill allows better curve fitting and is suggested for movements involving larger displacement like walking (Howarth and Callaghan. 2010; Gomes et al. 2021). The pattern fill and the rigid body fill methods are majorly dependent on the bone structure. Pattern fill requires at least two existent markers to estimate the trajectory, while rigid body fill requires at least three markers. Despite the enhanced efficacy brought by gap-filling methods, they still have limitations. Howarth and Callaghan (2010) reported that applying the spline method to gaps longer than 200 ms may lead to inaccurate results. Similarly, Gomes et al. (2021) found that the error with the spline method increased as the size of the gap increased, the pattern fill method presented more errors when more markers were missing, and errors with the rigid body fill method increased with both listed factors. Previous studies recommended that researchers inspect the characteristics of the gap in the data and select the most suitable gap-filling method based on the movement types as well (Gomes et al. 2021).

5.2 Gait event detection algorithms

To further analyze stride-to-stride variance in gait, the continuously recorded walking motion is dissected into multiple gait cycles based on critical gait events, such as foot-strikes and foot-offs. Although the ground reaction force is considered the gold standard for detecting gait events (Hreljac and Marshall. 2000; Hansen et al. 2002; Zeni et al. 2008), force plates are not always available in laboratory and clinical settings. Therefore, scientists have developed alternatives based on the kinematic data which can be collected by accelerometers, gyroscopes, or optical motion capture systems, allowing a more versatile environment for gait analysis.

There are two major types of automatic gait event detection algorithms for marker-based MoCap systems: coordinate-based and velocity-based. The coordinate-based algorithms define the events based on the markers' position, such as the methods proposed by Zeni et al. (2008).

On the other hand, an example of velocity-based algorithms is Ghoussayni et al. (2004), who used the descending and ascending sagittal velocity of markers to estimate gait events. Both the methods mentioned above were verified by Bruening and Ridge (2014), showing promising estimations of foot-strike and foot-off. Pantall et al. (2012) investigated the accuracy of four event detection algorithms in sloped walking of cats, and the method based on the vertical acceleration and vertical velocity of the marker on the metatarsophalangeal joint for foot strike and foot off respectively showed the least absolute systematic error. While the method adapted from Zeni et al. (2008) did not stand out on either the timing of foot strike or foot off, it had the lowest random error of the four algorithms that were tested (Pantall et al. 2012).

Despite the advantages, the estimation can be affected by pathological gait patterns (Bruening and Ridge. 2014). Caron-Laramée et al. (2023) presented that the accuracy of detected foot-off timing improved as the walking speed increased. As a result, the researchers should consider the factors that have a potential influence on gait when applying automatic gait event detection algorithms.

5.3 Analysis of movement variability

Variability can be analyzed using continuous or discrete methods. The continuous method takes the entire biomechanics waveform into account, which provides a higher dimensional understanding of the behavior, while the discrete method focuses on a specific point on the waveform (Hamill et al. 1999; Baida et al. 2018). The traditional linear analysis methods (e.g. mean, standard deviation, and coefficient of variance) measure the amount of variability (Harbourne and Stergiou. 2009), but may mask the true complexity of human movements (Stergiou. 2004). Newell and Corcos. (1993) stated that quantifying movement variability by standard deviation only presented the degree of variability of a given system parameter. In contrast, the nonlinear methods (e.g. the Lyapunov exponent and approximate entropy) reveal the structure of variability and would be more suitable for investigating the complexity of movements (Stergiou. 2004; Harbourne and Stergiou. 2009).

Harbourne and Stergiou (2009) explained the differences between interpreting variability with linear and non-linear methods by comparing the output values of several signals (Figure 3). While the second signal shows higher regularity than the first one, the value of the range does not differ between them. In contrast, the fourth signal with similarly high repeatability acquires

a larger value of range. With approximate entropy (ApEn), the variability of the first and second signals can be differentiated and does not define the fourth signal as less regular than the second signal.

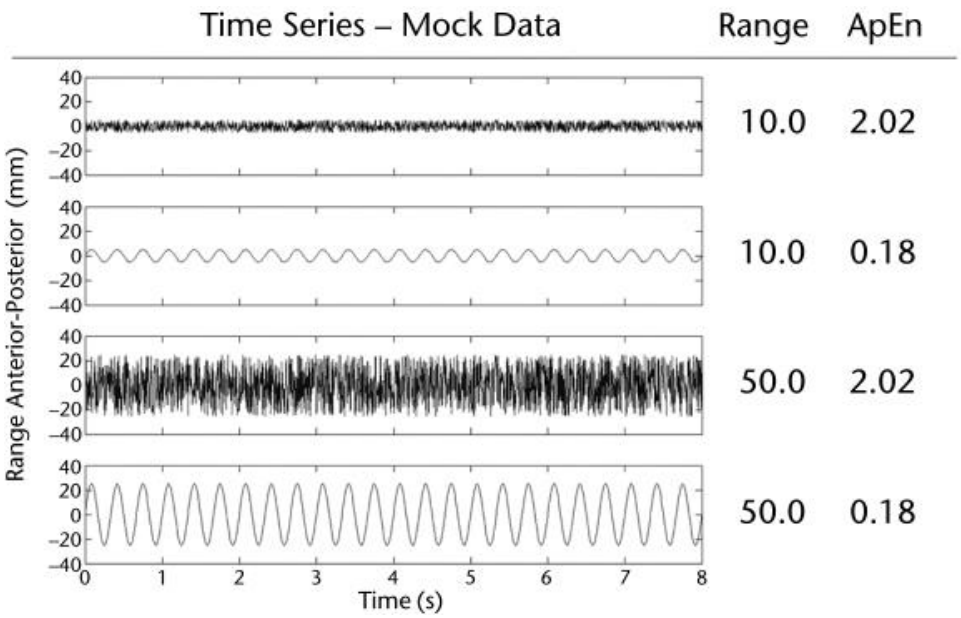

FIGURE 3. Comparison between values computed by the linear and non-linear method for four different signals. Adopted from Harbourne and Stergiou (2009).

Entropy originated from the field of thermodynamics and derived from which, approximate entropy was introduced to the analysis of biological data by Pincus (1991). The earlier study stated that ApEn quantifies the irregularity and unpredictability of fluctuations over time series data (Pincus and Goldberger. 1994). Yentes and Raffalt (2021) specified that the mathematics of entropy is associated with probability. As mathematics defines probability as the chances of the event to occur, the larger probability thus indicates lower randomness. In other words, the higher entropy value can be interpreted as having a lower probability of a certain pattern and a higher probability of a new or random one occurring in the movement system (Yentes and Raffalt. 2021).

The ApEn analysis is widely adopted to evaluate movement tasks and presents the result in a straightforward manner (Yentes et al. 2013; Raffalt et al. 2019). However, there is a mathematical issue within the nature of ApEn. When ApEn compared the vectors in the data, the reference vector is compared to itself as well to avoid the natural logarithm of zero, which may bias the result (Pincus and Goldberger. 1994; Richman and Moorman. 2000; Yentes and

Raffalt. 2021). The other single-scale entropy, sample entropy (SampEn) was therefore developed to overcome this problem (Richman and Moorman. 2000).

5.3.1 Mathematics of entropy

The standard unit of ApEn is bits, which range from 0 to 2. The mathematical descriptions of ApEn in the following paragraph are adopted from several literature sources (Pincus and Goldberger. 1994; Richman and Moorman. 2000; Yentes and Raffalt. 2021).

First, to compute ApEn, three input parameters have to be defined, which are the data points (N), the length of compared runs (m), and tolerance or threshold (r). The data points we have are $u(1)$, $u(2)$, …, $u(N)$, and the vector sequence is conducted from $x(1)$ to $x(N - m + 1)$, where $x_m(i)$ is defined as $[u(i), \ldots, u(i + m - 1)]$. The distance between two vectors, $x_m(i)$ and $x_m(j)$, is defined as $d[x_m(i), x_m(j)]$. In other words, the largest difference in the respective scalar component is regarded as the distance between $x_m(i)$ and $x_m(j)$. There will be $(N - m + 1)$ types of combinations of $x_m(i)$ and $x_m(j)$, including the situation that $i = j$. Repeating the above steps, we define the vector of $x_{m+1}(i)$, which is $[u(i), \ldots, u(i + (m + 1) - 1)]$, and the distance between the two vectors, that is $d[x_{m+1}(i), x_{m+1}(j)]$.

$$d[x_m(i), x_m(j)] = \max\{|u(i + k) - u(j + k)|: 0 \leq k \leq m - 1\}$$
$$d[x_{m+1}(i), x_{m+1}(j)] = \max\{|u(i + k) - u(j + k)|: 0 \leq k \leq m\}$$

The number of $d[x_m(i), x_m(j)]$ within r is presented as B_i, and the number of $d[x_{m+1}(i), x_{m+1}(j)]$ that is within r is A_i. The functions $C_i^m(r)$ and $C_i^{m+1}(r)$, which are average values of B_i and A_i respectively, are defined to reflect the conditional probability of the similarity between two observed runs of patterns.

$$C_i^m(r) = B_i\,(N - m + 1)^{-1}$$
$$C_i^{m+1}(r) = A_i\,(N - m)^{-1}$$

After the values of $C_i^m(r)$ and $C_i^{m+1}(r)$ are converted by natural logarithm, the function $\Phi^m(r)$ computed the average value of all $\ln [C_i^m(r)]$ $(1 \leq i \leq N - m + 1)$, likewise for $\Phi^{m+1}(r)$.

$$\Phi^m(r) = (N - m + 1)^{-1} \sum_{i=1}^{N-m+1} \ln [C_i^m(r)]$$

$$\Phi^{m+1}(r) = (N - m)^{-1} \sum_{i=1}^{N-m} \ln [C_i^{m+1}(r)]$$

Finally, ApEn(m, r, N) = $\Phi^m(r) - \Phi^{m+1}(r)$ is defined. To ensure that the outcome number remains positive, the negative ApEn value is adopted for further interpretation. The SampEn differs from the ApEn majorly in the last half of the calculation, where the $\Phi^m(r)$ is defined without the natural logarithm. As the self-matching condition is excluded ($i \neq j$), and only the first $N - m$ vectors are included in the calculation, the number of $d[x_m(i), x_m(j)]$ within r divided by the number of comparisons (N – m – 1) is presented as $B_i^m(r)$. The $B^m(r)$ is further defined, and the same principles are applied to form $A^m(r)$ where A_i represents the number of $d[x_{m+1}(i), x_{m+1}(j)]$ within r.

$$B_i^m(r) = B_i (N - m - 1)^{-1}$$
$$A_i^m(r) = A_i (N - m - 1)^{-1}$$
$$B^m(r) = (N - m)^{-1} \sum_{i=1}^{N-m} B_i^m(r)$$
$$A^m(r) = (N - m)^{-1} \sum_{i=1}^{N-m} A_i^m(r)$$

Lastly, when the N is limited, the SampEn(m, r, N) = $-\ln [A^m(r)/B^m(r)]$. If $A^m(r)$ or $B^m(r)$ is zero, it means that the pattern within the data is completely random and will result in an infinitely large number of SampEn.

5.3.2 Considerations when choosing parameters

The selection of the parameters for entropy computation is important as it may lead to different results. Several studies have discussed the guidelines for choosing proper parameters according to the study design.

Pincus and Goldberger (1994) concluded that N = 1000, m = 2, and r = 0.1 to 0.25 multiplying SD of the data set yield meaningful statistics. Theoretically, the larger N is preferred for conducting ApEn analysis since the result is sensitive to the parameters when the data length is short ($N \leq 200$) (Yentes et al. 2013). When determining the amount of data points, considering the constraints of the study design and the characteristics of the movement to be analyzed is important as well (Yentes et al. 2013). Raffalt et al. (2019) compared the kinematic data collected with several sampling frequencies and concluded that the increase in sampling

frequency resulted in lower SampEn. Moreover, the data points within a single gait cycle had a greater influence on the results of SampEn than the number of strides (Raffalt et al. 2019).

For discrete data analysis, m = 2 or 3 provides reasonable results, while it may not be suitable for continuous data analysis (Yentes and Raffalt. 2021). For instance, the pattern of the joint angle in gait generally repeats every gait cycle, so comparing the patterns of neighboring data points may only reveal the variance within the gait cycle rather than between cycles (McCamley et al. 2018). If the study aims to compare the joint angle between cycles, normalizing the data within each cycle to 100 points and applying m = 99 or 100 would be more appropriate (Yentes and Raffalt. 2021). The other way suggested by previous articles is to apply a lag to the data set when m remains as 2 or 3 (McCamley et al. 2018; Yentes and Raffalt. 2021). In this case, the $x_3(1)$ would possibly be [$u(1)$, $u(101)$, $u(201)$] and compared to $x_3(2)$ = [$u(2)$, $u(102)$, $u(202)$].

The parameter r considerably affects the result of ApEn and SampEn by determining the tolerated difference between two compared vectors (Yentes et al. 2018). A larger r allows more compared vectors in a time series to be recognized to have similar patterns, and vice versa. Lu et al. (2008) proclaimed that the selected r value should be able to provide the maximum ApEn while inheriting r = 0.1 – 0.2 times standard deviation, as most studies did, might not fulfill this task depending on the data. Aside from determining r by the standard deviation (rSD), a fixed constant is another option for setting a tolerance level (rConstant). Yentes et al. (2018) analyzed the step time variability of level ground walking and treadmill walking with ApEn and SampEn. They observed that, when comparing two groups with different standard deviations, rConstant may lead to a lower entropy value for the group with a lower standard deviation than rSD does (Yentes et al. 2018).

To conclude, the output entropy values are sensitive to chosen parameters, and the optimal practice is reporting entropy results of multiple combinations of parameters in an appendix, which allows not only transparency in methods but also the possibility for future scholars to compare between studies (Yentes and Raffalt. 2021). For example, if one adopts rSD as the parameter, r = 0.1, 0.2, 0.3 times the standard deviation should be examined (Yentes and Raffalt. 2021). For those choosing rConstant as the parameter, they should test the r from 0 to n*(1/sampling rate), where n is iterated (Yentes et al. 2018). The target is to find out the r value, above or below which the tendency of differences between data sets becomes consistent.

6 PURPOSE OF THE STUDY

To have a thorough understanding of how the sensorimotor strategy adapts to perturbations from the environment, stride-to-stride joint angle variability of downhill walking should be examined. Since previous studies investigated the stride-to-stride joint angle variability of sloped walking with linear methods instead of non-linear methods, the complexity of movements remains unclear. Therefore, a non-linear method, sample entropy, will be applied to acquire the complexity of movement. Moreover, the previous studies conducted the entropy analysis with the commonly adopted vector length (m=2), while this selected parameter may not be optimal for presenting the biological meaning of the continuous joint angle data of gait (Yentes and Raffalt. 2021). The feasibility of applying an elongated vector that accommodates the entire gait cycle should be examined.

As a result, the purpose of the study was two-fold. First, the stride-to-stride joint angle variability of the hip, knee, and ankle on the sagittal plane when walking across different inclinations, including uphill and downhill, was investigated. Second, the analysis was conducted via a linear and a non-linear method to reveal the amount and the structure of stride-to-stride sagittal-plane joint angle variability respectively.

Based on the previous research, the sensorimotor system is subject to more perturbations when walking on slopes compared to level ground (Sheehan and Gottschall. 2012; Dewolf et al. 2020), and the sensorimotor strategy tends to respond and counteract perturbations by increasing sagittal-plane joint angle variability (Alkjær et al. 2012; Estep et al. 2018; Mohr et al. 2023). As a result, in this study, it was hypothesized that lower limb sagittal-plane joint angle variability would be higher as inclination increased in either a positive or negative direction. Furthermore, significant differences were expected at the ±12° slope where the critical changes occur in biomechanics (Kawamura et al. 1991).

7 METHODS

7.1 Participants

The data was collected from participants aged 18-45 years old for men and 18-55 years old for women, who were able to understand the information in Finnish or English language. The exclusion criteria were: (1) having a musculoskeletal injury that is acute or happened less than 6 months before the measurements; 2) having an acute illness such as flu or fever; (3) having a chronic disorder that would affect running techniques; 4) being diagnosed or in moderate to high risk of cardiovascular disorders; (5) having a respiratory disorder, except for endurance athletes whose asthma is under medical control; (6) pregnant.

In total, 57 participants were recruited. Informed consent was obtained for all participants, as approved by the local ethical committee, in accordance with the Declaration of Helsinki. To ensure optimal visibility for the motion-capture system, participants were required to wear tight, short sports outfits that did not occlude the markers during measurements. They were instructed to wear comfortable sports shoes and a pair of pressure sensor insoles were inserted into the shoes' of the participants. The reflective markers were attached to the participants with double-sided tape. A set of inertial module sensors for bilateral lower limbs were mounted on the participants' pelvis, thighs, shanks, and feet. The data acquired from the inertial module sensors and the pressure sensor insoles were arranged for other research purposes and would not be analyzed for this study.

7.2 Protocol overview

The participants walked on a treadmill (OJK-1, Telineyhtymä, Kotka, Finland) at a constant speed with inclines of 0°, ±2°, ±4°, ±6°, and ±12°, and kinematic information was collected with an 8-camera MoCap system (Vicon Motion Systems Ltd., Oxford, UK), with a sampling rate of 200Hz. Before the measurement started, the MoCap system was calibrated to locate the global coordinate system and acquire the optimal capture volume. A motorized treadmill which allowed to adjust inclinations from +20° to -20° was used in this study. A digital inclinometer was positioned on the treadmill to confirm the incline level.

7.2.1 Anthropometric measurement

The anthropometric measurements follow the subject measurement instructions from the Vicon Nexus User Guideline (Vicon Motion Systems Ltd., Oxford, UK). Body mass and height were measured both with and without shoes. Leg length was measured with a tape measure from the anterior prominence of the anterior superior iliac crest (ASIS) to the medial malleolus when the participant stood straight. The width of the knee and ankle joints was measured with a digital caliper. The width of the knee joint was measured from the lateral femoral condyle to the medial femoral condyle, and the ankle joint width was from the lateral malleolus to the medial malleolus.

7.2.2 Marker placement

The marker placement followed the Plug-in-Gait lower body model (Vicon Motion Systems Ltd., Oxford, UK) (16 markers), with 10 additional markers placed to enhance the tracking of the segment. There were 26 reflective markers in total on the pelvis, thighs, knees, shins, ankles, and feet on both sides. The labels of the markers are listed in Table 1 and the placement is demonstrated in Figure 4.

TABLE 1: Marker placement

Label	**Placement**
LASI / RASI	The prominence of the anterior superior iliac crest.
LPSI / RPSI	The prominence of the posterior superior iliac crest
LTHI / RTHI	The upper or lower one-third of the lateral thigh. The markers on both sides should be at different levels of height.
LKNE / RKNE	The lateral condyle of the femur.
LMKNE / RMKNE	The medial condyle of the femur.
LTIB / RTIB	The upper or lower one-third of the lateral shin. The markers on both sides should be at different levels of height.
LANK / RANK	The lateral malleolus of the fibula.

LMANK / RMANK	The medial malleolus of the tibia.
LLANK2 / RLANK2	The trochlear process on the calcaneus. *
LMANK2 / RMANK2	The sustentaculum tali on the calcaneus. *
LHEE / RHEE	The tuberosity of the calcaneus and at the same level as the TOE marker. *
LTOE / RTOE	The metatarsophalangeal joint of the second toe. *
LHLUX / RHLUX	The distal phalangeal of the first toe. *

*The anatomical bony landmarks were palpated from the outer layer of the shoes, and markers were placed on the surface of the shoes instead of the skin.

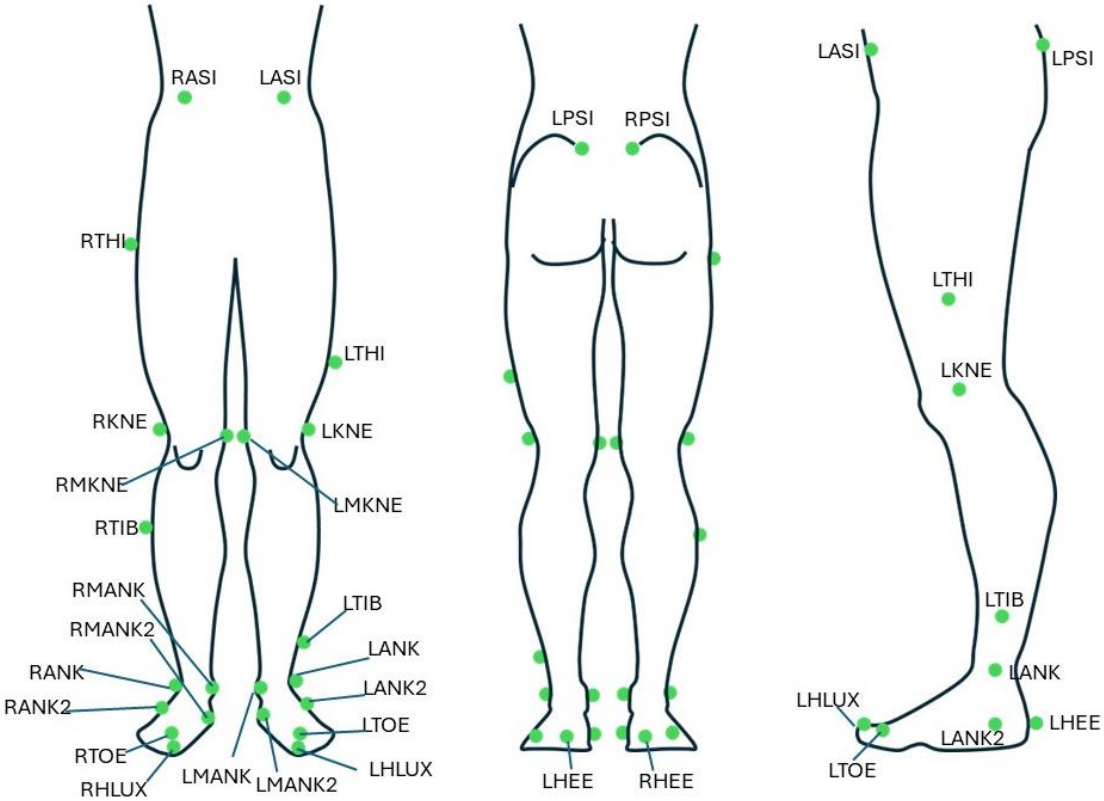

FIGURE 4. Marker placement on the lower limbs. From left to right, the views are from the front, back, and left lateral sides of the lower limbs, respectively.

7.3 Testing procedures

The participants wore a safety harness throughout the measurement and were instructed to maintain their position around the center of the capture volume. The researchers visually inspected the reflective markers on the monitor to ensure optimal visibility and adjusted them when needed. Before the measurement started, the MoCap system recorded the participants standing in the anatomical position and T-pose for Vicon calibration.

At the beginning of the measurement, the participants went through a 5.5-minute walking familiarization on the treadmill at a self-selected speed. The speed was raised and lowered in increments of 0.5 km/h during the familiarization to determine each participant's most natural walking speed for all subsequent trials.

One minute of walking allowed for the recording of at least 100 steps for analysis. Each walking trial was recorded for at least 1.5 minutes with the first 30 seconds at the beginning of every trial discarded to exclude unstable gait. Therefore, for the major tasks of this study, participants walked for 3.5 minutes at all inclinations except ±12°, where they walked for 1.5 minutes. The extended recording duration served another study purpose. The participants first walked at the speed determined during the familiarization and ±0.5 km/h of the selected speed at 0° inclination, and the order for different speeds was randomized. For walking at all inclinations, the participants maintained the selected speed, with the order for ±2°, ±4°, and ±6° inclines randomized. The ±12° inclines were executed after completing the other lower inclinations. For the participants who subjectively reported a strenuous feeling for the steepest conditions, the speed was 0.5 km/h slower than the selected speed. To eliminate the effect of changing speed on kinematics, only the participants who walked at a constant speed for all trials were included for further analysis. The treadmill was stopped and re-started for every new trial.

7.4 Data processing

Motion data was first processed with the Nexus software (v2.11, Vicon Motion Systems Ltd., Oxford, UK). After labeling the markers according to the Plug-in-Gait lower body model, gaps in the motion capture data that were shorter than 200 frames were filled through the built-in gap-filling functions in Nexus software. Next, data were processed with a dynamic Plug-in-Gait model, and the processed c3d files were exported to MATLAB software (version R2023a, Mathworks Inc., MA, USA). Custom code for MATLAB software was employed for estimating gait events and extracting joint angles data. The first 30 seconds of each walking trial were

discarded, and the joint angles of 40 consecutive gait cycles were saved in CSV format for further analysis. Custom Python code was executed on Spyder IDE (version 5.4.5) under the environment provided by Anaconda Navigator (version 2.5.0, Anaconda Inc., TX, USA) to perform further analysis.

7.4.1 Gait event detection

To estimate gait events, a set of custom MATLAB codes was used, which was modified from the work of Visscher et al. (2021) and was based on the method proposed by previous studies (Zeni et al. 2008; Pantall et al. 2012; Caron-Laramée et al. 2023). The functions from the Biomechanical Toolkit package (Barré and Armand. 2014) were adopted to extract marker trajectories. All marker trajectories were filtered with a 4^{th}-order low-pass Butterworth filter with a 7 Hz cutoff frequency. A virtual sacrum marker was formed from the midpoint of LPSI and RPSI markers. The horizontal distance between the sacrum and foot markers was calculated. By applying the find-peaks function, the time points where the maximum and minimum horizontal distance occurred were identified as heel strikes and foot-offs respectively. In the algorithm, the heel marker was selected for detecting heel strikes, and the hallux marker, suggested by Bruening and Ridge (2014), was used for foot-offs. Besides, a threshold of at least 40 frames (200 ms) between two consecutive events was set to reduce false positives. The frame numbers where the gait events occurred were listed in CSV files. Custom Python code was further applied to calculate spatiotemporal parameters, including stride length, step length, cadence, stride time, step time, stance duration, swing duration, proportion of stance phase, and proportion of swing phase for both left and right side (Appendix 1).

To verify that the algorithm estimated gait events at inclines with reasonable accuracy, trials of 5 participants were randomly selected, and 10 consecutive gait events at +12° and -12° of inclination were determined by visual inspection. The differences between the manual and the automatic method were calculated in milliseconds.

7.4.2 Joint angle variability analysis

To investigate stride-to-stride variability, filtering the marker trajectories was avoided since it might eliminate subtle but important biological information (Georgoulis et al. 2006). The joint angles on the sagittal plane for each trial were extracted with the Biomechanical Toolkit (Barré

and Armand. 2014), normalized to 100 data points for each gait cycle in MATLAB, and exported to CSV files. The joint angle fluctuations were plotted with the percentage of the gait cycle as the x-axis, and joint angles in degree as the y-axis. If any outliers and atypical patterns that did not seem to be biological were presented in the trial, the original movement recordings were reviewed. The trials that showed oscillating or flashing markers were categorized as trials with computational artifacts. If adjusting the interested frame zone forward could skip the section of computational artifacts, the adjusted trial was included for further analysis. Otherwise, it was excluded.

The sample entropy of 4,000 data points for each trial was computed through the function in the AntroPy package (Vallat. 2021) on Python. Two different lengths of vectors (m=2 and m=99) were examined. For m=2, r=0.1, 0.15, 0.2, 0.25, and 0.3 were applied, and the output with r=2 is presented in the results. For m=99, the r was first iterated from 0.2 to 4.5 on the right ankle joint to find a relatively consistent state of SampEn outputs. Later, the r=3.5 – 5.0, with intervals of 0.05, was applied to all investigated joints. The results of m=99 and r=4.5 are presented in the next chapter. The results calculated with additional r values not reported in the thesis are attached in the appendix.

The linear method was adapted from Sarvestan et al. (2021). The standard deviation of joint angle data at each percentage of gait cycles was calculated. The standard deviation values of each percentage of the 40 gait cycles were summed and averaged to present the overall variability throughout the stride. The output via the linear method is hereafter referred to as MeanSD.

7.5 Statistical analysis

The statistical analysis was conducted via Jamovi 2.3.26 Desktop (The Jamovi project. 2023). The alpha level for the examined data was set at 0.05. The spatiotemporal parameters and the stride-to-stride hip, knee, and ankle sagittal-plane joint angle variability on both the left and right sides were grouped according to the inclinations. Shapiro-Wilk tests were run to examine the normality of data in all groups. The null hypothesis was accepted for all spatiotemporal parameters across all inclinations, indicating normal distributions. In contrast, the null hypothesis was rejected for sagittal-plane joint angle variability of some inclinations. Therefore, a parametric repeated measures analysis of variance (ANOVA) was applied to investigate the

effect of inclinations on spatiotemporal parameters. The repeated measures ANOVA compared each spatiotemporal parameter across all inclinations. Post-hoc tests with Bonferroni correction were used to compare level and sloped walking. Alternatively, a non-parametric repeated measures ANOVA, the Friedman test, was applied to examine the effect of inclinations on the sagittal-plane joint angle variability by comparing the joint angle variability of each joint on the left and right side across all inclinations. The post-hoc pairwise comparison was conducted using the Durbin-Conover test to investigate the differences between inclinations.

8 RESULTS

8.1 Participant characteristics

Seven participants were excluded due to slower walking speeds at the steepest inclinations, and fifteen were excluded for extended marker occlusions (over 200 frames) or missing mandatory markers throughout the trial. The trial order for three participants was not clearly documented, and data for two participants were missing. Finally, thirty participants were included in the analysis. Participants' characteristics are summarized in Table 2.

Table 2. Participants' characteristics (n=30)

male=17, female=13

	Mean		SD
Age	34.2	±	7.6
Mass (kg)	72.5	±	12.8
Height (m)	1.75	±	0.09
Speed (m/s)	1.54	±	0.12

After inspecting the joint angle curves, a few trials were excluded due to artificial-like results arising from inaccurate estimation of the gap-filling algorithms and mislabeling of markers. Consequently, the number of participants included for the lower limb sagittal-plane joint angle variability was 21 for the left side and 28 for the right side.

8.2 Comparison between gait event algorithms and visual inspection

The negative mean value indicated that the gait event detection algorithm predominantly showed premature estimations among the FS and FO at +12° and -12° conditions compared to the visual inspection. The algorithm provided more accurate estimations for FO than for FS. The mean value, standard deviation, range, and mean absolute error (MAE) are listed in Table 3 and Figure 5.

TABLE 3. Differences between gait-event-detection algorithm and visual inspection

Inclination	+12		-12	
Event	FS	FO	FS	FO
Mean (ms)	-10.0	-0.6	-11.9	-5.2
SD (ms)	6.39	5.68	7.95	7.62
Median (ms)	-25	-10	-30	-20
Range (ms)	30	25	35	40
MAE (ms)	10.4	4.2	12.1	7.2

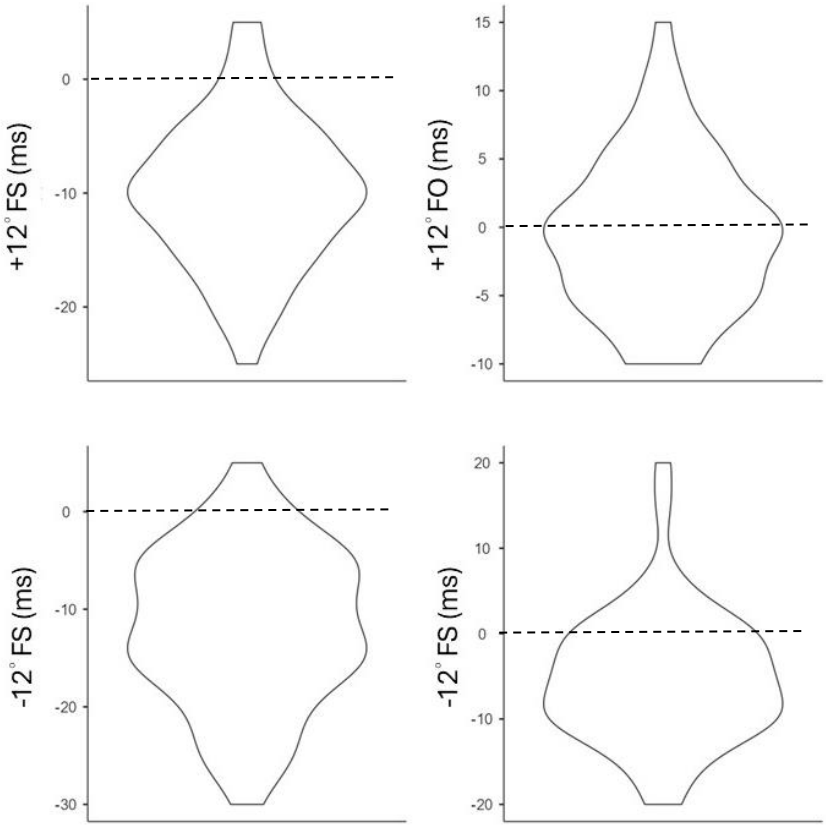

FIGURE 5. The violin plot presents the differences between visual inspection and the gait event detection algorithm and their respective distributions.

8.3 Spatiotemporal parameters

The repeated measures ANOVA revealed significant effects of inclinations on the spatiotemporal parameters, including the stride time, step time, stride length, step length, cadence, stance duration, swing duration, proportion of stance phase, and proportion of swing phase for both sides, as detailed in Table 4.

TABLE 4. Effect of inclination on spatiotemporal parameters (n=30)

	F	df	p	η^2
Left stride length	41.9	8, 323	<.001*	0.164
Right stride length	41.9	8, 232	<.001*	0.164
Step length	36.4	8, 232	<.001*	0.167
Cadence	34.4	8, 232	<.001*	0.230
Left stride time	41.4	8, 323	<.001*	0.207
Right stride time	41.5	8, 232	<.001*	0.207
Step time	36.5	8, 232	<.001*	0.213
Left stance duration	54.2	8, 232	<.001*	0.229
Right stance duration	51.2	8, 232	<.001*	0.230
Left swing duration	23.7	8, 232	<.001*	0.181
Right swing duration	22.7	8, 232	<.001*	0.159
Left stance phase	78.0	8, 232	<.001*	0.364
Right stance phase	53.4	8, 232	<.001*	0.318

F: F-value
df: degrees of freedom
η^2: effect size
*indicates significant effects of inclinations

The post-hoc tests showed significant differences in spatiotemporal parameters when comparing level walking to various slopes. The stride length of both sides and the step length significantly decreased at inclines of -12°, -6°, -4°, and +12°. The cadence significantly increased at inclines of -12°, -6°, -4°, and +12°. The step and stride time of both sides significantly decreased at inclines of -12°, -6°, -4°, and +12°, with the left stride time also showing a significant decrease at a -2° incline. The stance phase duration of both sides significantly decreased at all downhill conditions and at a +12° incline. In contrast, the swing phase duration of both sides decreased significantly only at inclines of -12° and +12°. The proportion of the stance phase significantly reduced at all the downhill slopes, although no significant changes were observed during the uphill walking (Table 5).

TABLE 5. Spatiotemporal parameters across inclinations (n= 30)

Inclination (°)		-12	-6	-4	-2	0	+2	+4	+6	+12
Left stride length (m)	Mean	1.41	1.50	1.53	1.54	1.56	1.56	1.56	1.55	1.46
	SD	0.14	0.11	0.11	0.11	0.11	0.11	0.10	0.11	0.99
	$p_{bonferroni}$	<.001*	<.001*	<.001*	0.059		1.000	1.000	1.000	<.001*
Right stride length (m)	Mean	1.41	1.50	1.53	1.54	15.6	1.56	1.56	1.55	1.46
	SD	0.14	0.11	0.11	0.11	0.11	0.11	0.10	0.11	0.99
	$p_{bonferroni}$	<.001*	<.001*	<.001*	0.064		1.000	1.000	1.000	<.001*
Step length (m)	Mean	0.70	0.75	0.76	0.76	0.77	0.77	0.77	0.76	0.72
	SD	0.07	0.06	0.05	0.06	0.05	0.06	0.05	0.05	0.05
	$p_{bonferroni}$	<.001*	<.001*	0.015*	0.933		1.000	1.000	0.200	<.001*
Cadence (1/min)	Mean	134	125	122	122	120	120	121	122	129
	SD	11.5	7.64	6.66	6.74	5.87	6.83	7.56	7.64	9.8
	$p_{bonferroni}$	<.001*	<.001*	0.014*	0.879		1.000	1.000	0.202	<.001*
Left Stride time (s)	Mean	0.92	0.98	0.99	1.00	1.01	1.01	1.01	1.00	0.95
	SD	0.08	0.06	0.05	0.05	0.05	0.06	0.06	0.07	0.07
	$p_{bonferroni}$	<.001*	<.001*	<.001*	0.048*		1.000	1.000	1.000	<.001*
Right Stride time (s)	Mean	0.92	0.98	0.99	1.00	1.01	1.01	1.01	1.00	0.95
	SD	0.08	0.06	0.05	0.05	0.05	0.06	0.06	0.07	0.07
	$p_{bonferroni}$	<.001*	<.001*	<.001*	0.051		1.000	1.000	1.000	<.001*
Step time (s)	Mean	0.45	0.48	0.49	0.50	0.50	0.50	0.50	0.49	0.47
	SD	0.04	0.03	0.03	0.03	0.03	0.03	0.03	0.03	0.04
	$p_{bonferroni}$	<.001*	<.001*	0.019*	0.871		1.000	1.000	0.273	<.001*
Left stance duration (s)	Mean	0.58	0.62	0.64	0.64	0.66	0.66	0.66	0.65	0.62
	SD	0.06	0.04	0.04	0.04	0.04	0.04	0.04	0.05	0.05
	$p_{bonferroni}$	<.001*	<.001*	<.001*	0.001*		1.000	1.000	1.000	<.001*
Right stance duration (s)	Mean	0.58	0.62	0.64	0.65	0.66	0.66	0.66	0.65	0.62
	SD	0.05	0.04	0.04	0.04	0.04	0.04	0.04	0.05	0.05
	$p_{bonferroni}$	<.001*	<.001*	<.001*	0.010*		1.000	1.000	1.000	<.001*
Left swing duration (s)	Mean	0.34	0.35	0.36	0.36	0.36	0.35	0.36	0.35	0.33
	SD	0.02	0.02	0.01	0.01	0.01	0.02	0.02	0.02	0.02
	$p_{bonferroni}$	0.006*	1.000	1.000	1.000		1.000	1.000	1.000	<.001*
Right swing duration (s)	Mean	0.34	0.35	0.35	0.35	0.36	0.35	0.36	0.35	0.33
	SD	0.03	0.02	0.02	0.01	0.01	0.02	0.02	0.02	0.02
	$p_{bonferroni}$	0.003*	1.000	1.000	1.000		1.000	1.000	1.000	<.001*
	Mean	63.0	63.7	64.0	64.3	64.8	64.8	64.8	64.8	64.9

Left stance phase (%)	SD	1.2	0.8	0.7	0.8	0.7	0.8	0.8	0.8	0.8
	$p_{bonferroni}$	<.001*	<.001*	<.001*	<.001*		1.000	1.000	1.000	1.000
Right stance phase (%)	Mean	63.2	64.0	64.3	64.6	64.9	65.0	64.9	64.8	64.9
	SD	1.1	0.8	0.8	0.7	0.7	0.8	0.8	0.8	0.8
	$p_{bonferroni}$	<.001*	<.001*	<.001*	0.005*		1.000	1.000	1.000	1.000

*indicates a significant difference compared to level ground walking

8.4 Joint angle variability

One participant's stride-to-stride lower limb sagittal-plane joint angle for the consecutive 40 strides was plotted in Appendix 2 to provide a visualized example of the stride-to-stride joint angle variability.

8.4.1 MeanSD

MeanSD represented the sagittal-plane joint angle variability using the linear method. The Friedman test of MeanSD showed that inclinations had significant effects on the variability of all lower limb joint angles on both the left and right sides (Table 6).

TABLE 6. Effect of inclination on joint angle variability (MeanSD)

	Joint	χ^2	df	p
Left (n=21)	Hip	124	8	<.001*
	Knee	119	8	<.001*
	Ankle	102	8	<.001*
Right (n=28)	Hip	166	8	<.001*
	Knee	162	8	<.001*
	Ankle	151	8	<.001*

χ^2: chi-squared
df: degrees of freedom
*indicates significant effects

Compared to level walking, the left hip sagittal-plane joint angle variability was significantly higher at all downhill, +6°, and +12° inclines. The left knee sagittal-plane joint angle variability was significantly higher at -12°, -6°, -4°, +6°, and +12° inclines. Similarly, the left ankle

sagittal-plane joint angle variability was significantly higher at -12°, -6°, -4°, +6°, and +12° inclines. (Table 7 and Figure 6).

TABLE 7. MeanSD of left lower limb joint angle across inclinations (n = 21)

Inclination (°)	Hip			Knee			Ankle		
	Mean	SD	p	Mean	SD	p	Mean	SD	p
-12	1.90	0.401	<.001*	2.60	0.499	<.001*	1.59	0.253	<.001*
-6	1.37	0.325	<.001*	2.01	0.343	<.001*	1.28	0.265	<.001*
-4	1.15	0.243	<.001*	1.71	0.313	<.001*	1.14	0.222	0.006*
-2	1.01	0.174	0.001*	1.48	0.280	0.203	1.03	0.223	0.792
0	0.92	0.158		1.40	0.216		1.02	0.150	
+2	0.90	0.170	0.454	1.40	0.356	0.610	1.00	0.210	0.175
+4	0.98	0.214	0.088	1.51	0.248	0.011*	1.05	0.145	0.693
+6	1.06	0.225	<.001*	1.59	0.298	<.001*	1.14	0.151	<.001*
+12	1.61	0.434	<.001*	1.98	0.420	<.001*	1.47	0.380	<.001*

*indicates a significant difference compared to level ground walking

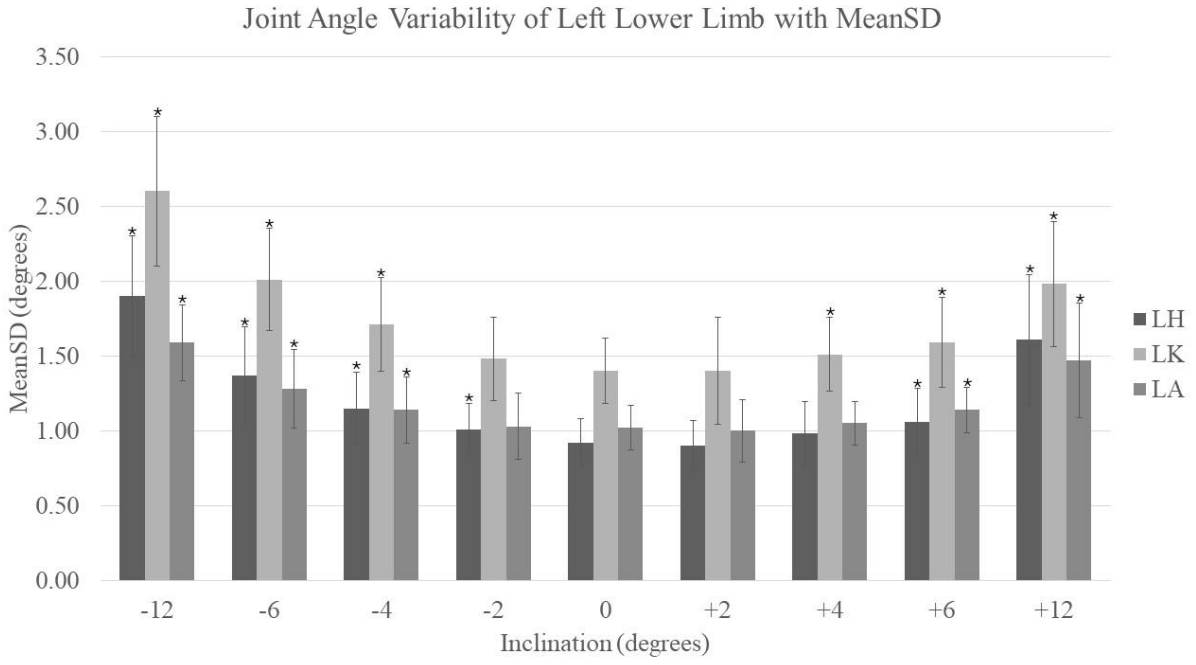

FIGURE 6. The sagittal-plane joint angle variability of the left hip (LH), left knee (LK), and left ankle (LA) computed with the linear method. * indicates significant differences compared to level walking ($p<0.05$).

The right hip, knee, and ankle sagittal-plane joint angle variability with MeanSD was significantly higher at all the downhill and uphill conditions, except for +2°. (Table 8 and Figure 7).

Table 8. MeanSD of right lower limb joint angle across inclinations (n = 28)

	Hip			Knee			Ankle		
Inclination (°)	Mean	SD	p	Mean	SD	p	Mean	SD	p
-12	1.89	0.415	<.001*	2.56	0.504	<.001*	1.84	0.329	<.001*
-6	1.31	0.309	<.001*	2.01	0.381	<.001*	1.46	0.317	<.001*
-4	1.19	0.300	<.001*	1.81	0.364	<.001*	1.34	0.311	<.001*
-2	1.02	0.159	<.001*	1.54	0.266	<.001*	1.19	0.265	0.007*
0	0.95	0.212		1.42	0.270		1.13	0.284	
+2	0.92	0.182	0.122	1.44	0.336	0.927	1.08	0.251	0.113
+4	1.00	0.189	0.040*	1.54	0.241	<.001*	1.16	0.194	0.022*
+6	1.09	0.221	<.001*	1.61	0.289	<.001*	1.26	0.206	<.001*
+12	1.64	0.435	<.001*	1.98	0.413	<.001*	1.58	0.302	<.001*

*indicates a significant difference compared to level ground walking

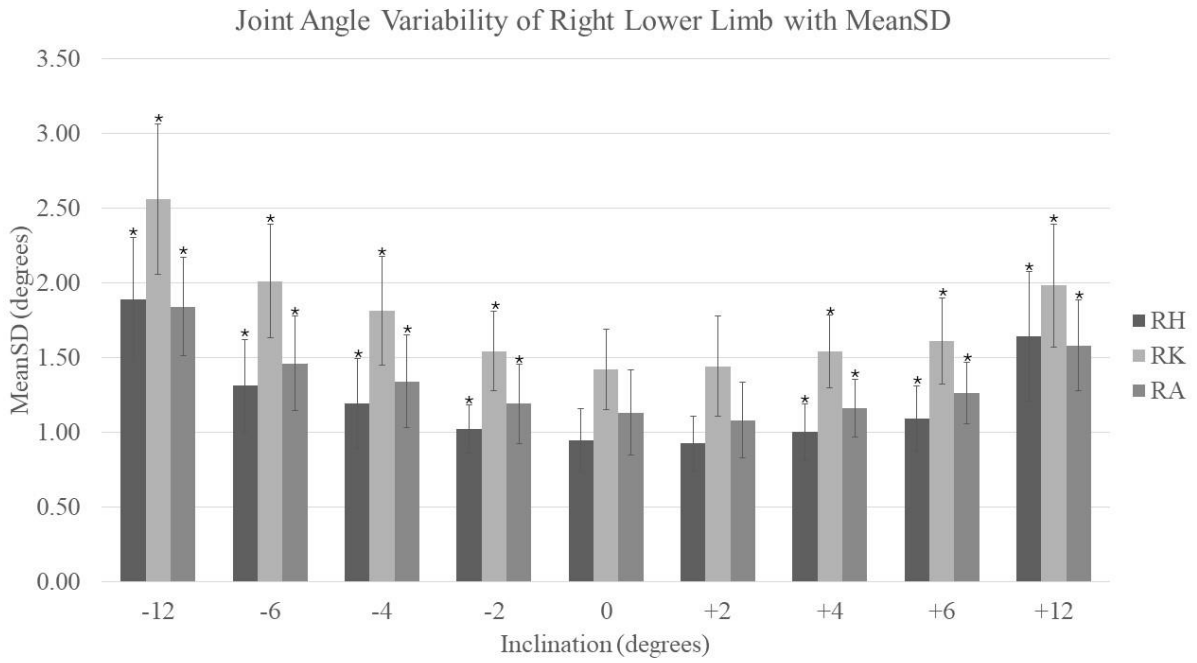

FIGURE 7. The sagittal-plane joint angle variability of the right hip (RH), right knee (RK), and right ankle (RA) computed with the linear method. * indicates significant differences compared to level walking ($p<0.05$).

8.4.2 SampEn (*m*=2)

The results of the Friedman test showed that the inclinations had significant effects on all lower limb sagittal-plane joint angle variability of both the left and right sides when computed with SampEn (*m*=2, *r*=0.2, *N*=4,000) (Table 9). The output SampEn at 0° and ±12° with the other tested tolerance levels is attached to Appendix 3.

TABLE 9. Effect of inclination on joint angle variability (SampEn with *m*=2, *r*=0.2)

	Joint	χ^2	df	p
Left (n=21)	Hip	109	8	<.001*
	Knee	67.8	8	<.001*
	Ankle	43.6	8	<.001*
Right (n=28)	Hip	142	8	<.001*
	Knee	124	8	<.001*
	Ankle	93.5	8	<.001*

χ^2: chi-squared
df: degrees of freedom
*indicates significant effects

The post hoc test showed that, compared to level ground, the left hip sagittal-plane joint angle variability was significantly higher on all downhill inclines and significantly lower at +4° and +6° inclines. The left knee sagittal-plane joint angle variability was significantly higher at -12°, -6°, -4°, and +12° inclines. Similarly, the left ankle sagittal-plane joint angle variability was significantly higher at the -12° incline. (Table 10 and Figure 8).

TABLE 10. SampEn (m=2, r=0.2) of left lower limb joint angle across inclinations (n = 21)

	Hip			Knee			Ankle		
Inclination (°)	Mean	SD	p	Mean	SD	p	Mean	SD	p
-12	0.867	0.120	<.001*	0.973	0.131	<.001*	0.801	0.097	<.001*
-6	0.795	0.094	<.001*	0.902	0.140	<.001*	0.715	0.086	0.127
-4	0.747	0.094	0.003*	0.865	0.130	0.037*	0.699	0.094	0.293
-2	0.738	0.094	0.024*	0.846	0.131	0.455	0.694	0.095	0.523
0	0.698	0.078		0.830	0.158		0.686	0.092	
+2	0.685	0.099	0.088	0.812	0.151	0.455	0.664	0.090	0.092
+4	0.629	0.082	<.001*	0.815	0.151	0.241	0.679	0.086	0.293
+6	0.625	0.088	<.001*	0.839	0.153	0.749	0.707	0.103	0.463
+12	0.701	0.126	0.781	0.931	0.143	<.001*	0.687	0.102	0.610

*indicates a significant difference compared to level ground walking

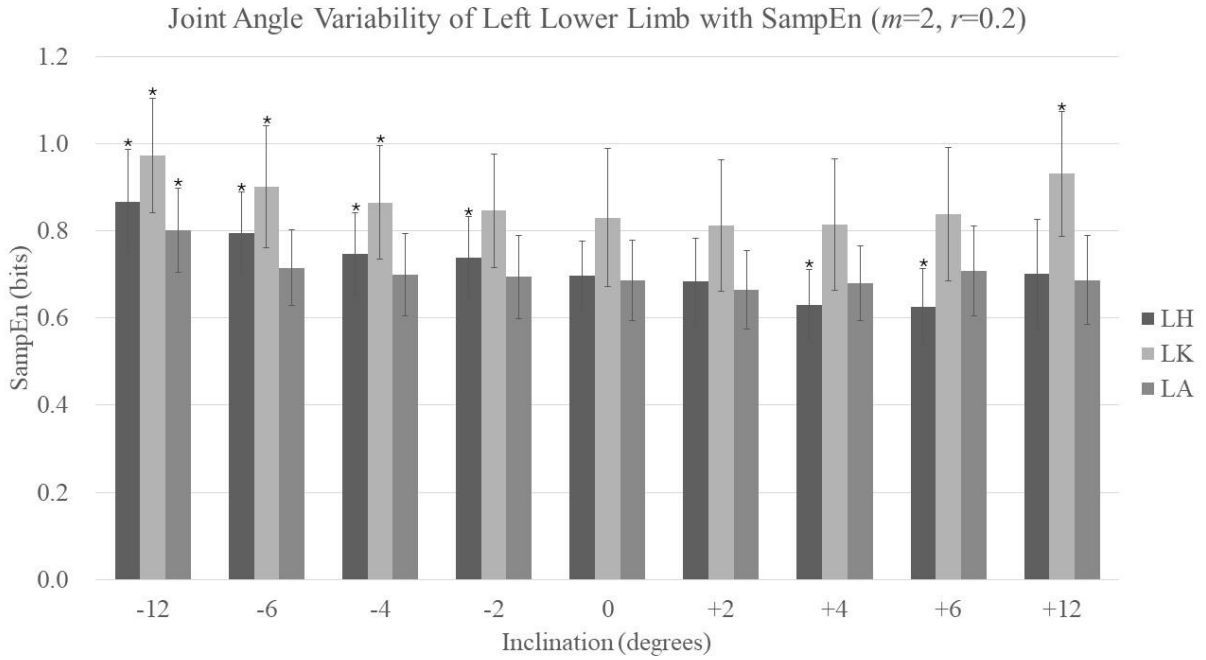

FIGURE 8. The sagittal-plane joint angle variability of the left hip (LH), left knee (LK), and left ankle (LA) computed with SampEn (*m*=2, *r*=0.2). * indicates significant differences compared to level walking ($p<0.05$)

The right hip sagittal-plane joint angle variability was significantly higher on all downhill inclines and significantly lower at +4° and +6° inclines. The right knee sagittal-plane joint angle variability was significantly higher at -12°, -6°, -4°, and +12° inclines, and significantly lower

at +4° incline. Similarly, the right ankle sagittal-plane joint angle variability was significantly higher on all downhill inclines and at the +12° incline. (Table 11 and Figure 9).

TABLE 11. SampEn (m=2, r=0.2) of right lower limb joint angle across inclinations (n = 28)

	Hip			Knee			Ankle		
Inclination (°)	Mean	SD	p	Mean	SD	p	Mean	SD	p
-12	0.822	0.106	<.001*	0.914	0.123	<.001*	0.902	0.090	<.001*
-6	0.767	0.099	<.001*	0.826	0.102	<.001*	0.808	0.118	<.001*
-4	0.732	0.088	<.001*	0.818	0.117	<.001*	0.778	0.109	<.001*
-2	0.707	0.086	0.001*	0.784	0.115	0.069	0.751	0.086	0.019*
0	0.663	0.075		0.753	0.111		0.730	0.082	
+2	0.642	0.098	0.107	0.738	0.106	0.229	0.719	0.079	0.900
+4	0.615	0.071	0.007*	0.727	0.096	0.018*	0.714	0.086	0.754
+6	0.595	0.078	<.001*	0.740	0.106	0.122	0.718	0.114	1.000
+12	0.664	0.104	0.453	0.820	0.114	<.001*	0.749	0.102	0.029*

*indicates a significant difference compared to level ground walking

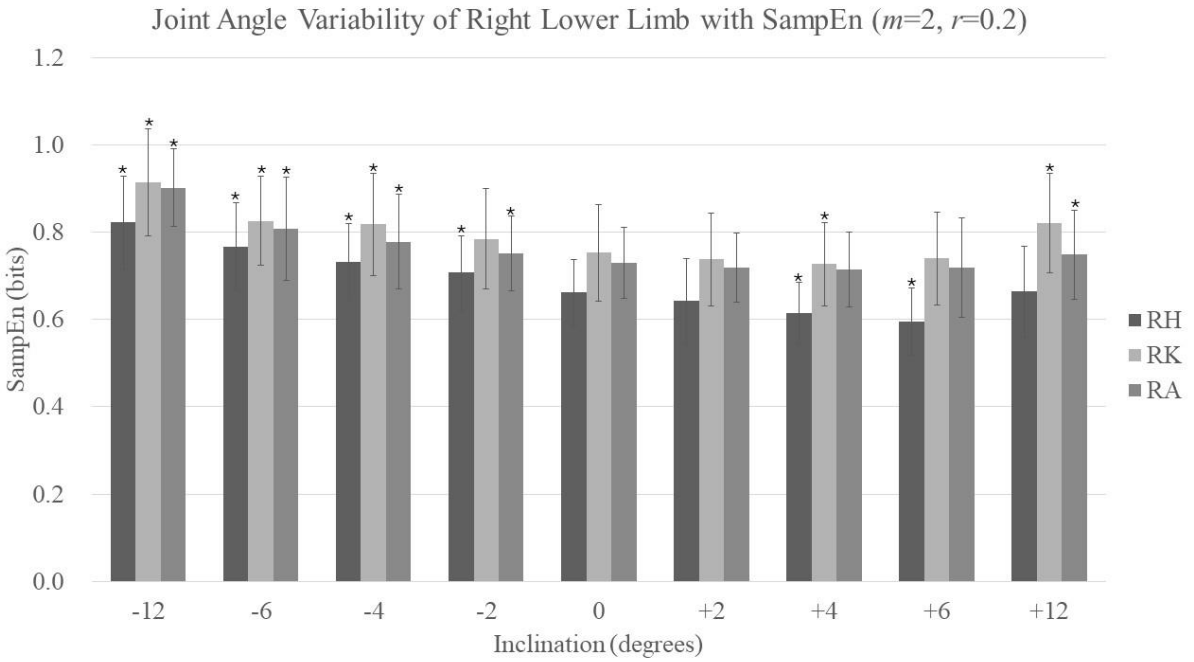

FIGURE 9. The sagittal-plane joint angle variability of the right hip (RH), right knee (RK), and right ankle (RA) computed with SampEn (*m*=2, *r*=0.2). * indicates significant differences compared to level walking ($p<0.05$).

8.4.3 SampEn (*m*=99)

The results of the Friedman test showed that the inclinations had significant effects on all lower limb sagittal-plane joint angle variability of both the left and right sides when computed with SampEn (*m*=99, *r*=4.5, *N*=4,000) (Table 12). The output SampEn at 0° and ±12° with the other tested tolerance levels is attached to Appendix 4.

TABLE 12. Effect of inclination on joint angle variability (SampEn with *m*=99, *r*=4.5)

	Joint	χ^2	df	p
Left (n=21)	Hip	124	8	<.001*
	Knee	120	8	<.001*
	Ankle	92.7	8	<.001*
Right (n=28)	Hip	167	8	<.001*
	Knee	155	8	<.001*
	Ankle	146	8	<.001*

χ^2: chi-squared
df: degrees of freedom
*indicates significant effects
*indicates significant effects

The post hoc test showed that, compared to level ground, the left hip sagittal-plane joint angle variability was significantly higher on all downhill inclines, as well as at +6° and +12° inclines. The left knee sagittal-plane joint angle variability was significantly higher at all inclines, except for +2°. Similarly, the left ankle sagittal-plane joint angle variability was significantly higher at -12°, -6°, -4°, and +12° inclines. The results are summarized in Table 13 and Figure 10.

TABLE 13. SampEn (m=99, r=4.5) of left lower limb joint angle across inclinations (n = 21)

	Hip			Knee			Ankle		
Inclination (°)	Mean	SD	p	Mean	SD	p	Mean	SD	p
-12	0.01140	0.00411	<.001*	0.02390	0.00638	<.001*	0.01420	0.00334	<.001*
-6	0.00633	0.00293	<.001*	0.01610	0.00306	<.001*	0.00956	0.00263	<.001*
-4	0.00466	0.00179	<.001*	0.01220	0.00357	<.001*	0.00826	0.00251	<.001*
-2	0.00357	0.00161	0.038*	0.00978	0.00266	0.026*	0.00730	0.00329	0.512
0	0.00300	0.00148		0.00852	0.00254		0.00664	0.00238	
+2	0.00284	0.00116	0.337	0.00856	0.00303	0.683	0.00632	0.00262	0.220
+4	0.00335	0.00133	0.488	0.00995	0.00273	0.015*	0.00648	0.00221	0.594
+6	0.00381	0.00163	<.001*	0.01110	0.00344	<.001*	0.00675	0.00190	0.566
+12	0.00716	0.00405	<.001*	0.01460	0.00541	<.001*	0.00961	0.00403	<.001*

*indicates a significant difference compared to level ground walking

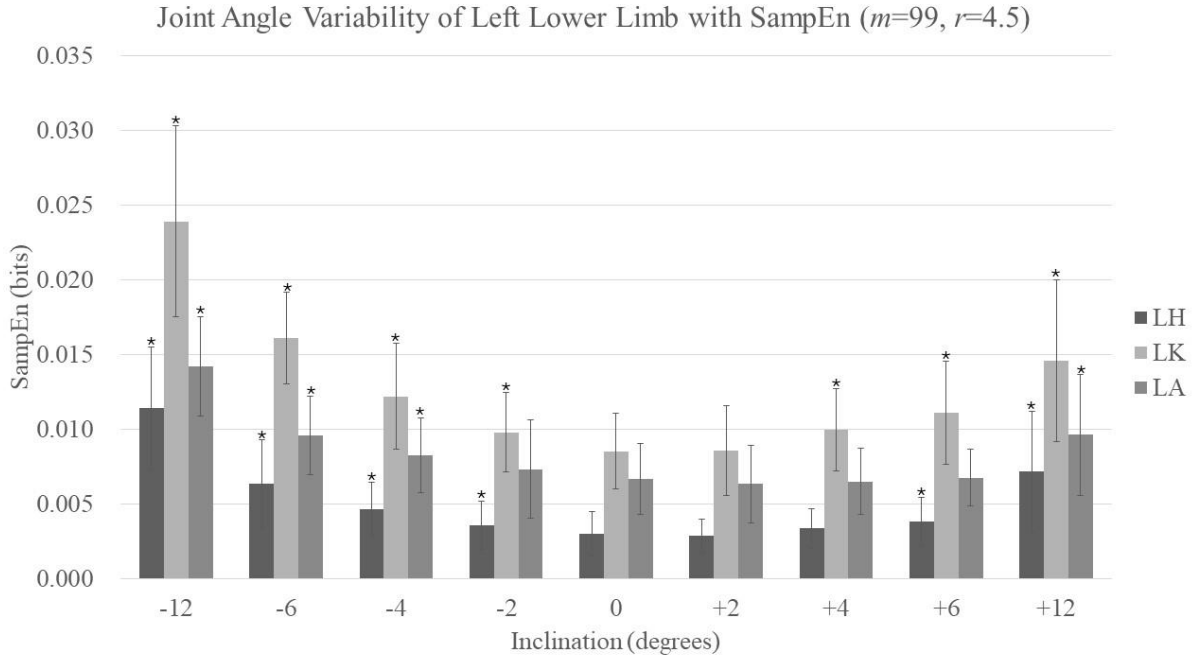

FIGURE 10. The sagittal-plane joint angle variability of the left hip (LH), left knee (LK), and left ankle (LA) computed with SampEn (*m*=99, *r*=4.5). * indicates significant differences compared to level walking.

The right hip and knee sagittal-plane joint angle variability were significantly higher on all downhill and uphill inclines, except for +2°. The right ankle sagittal-plane joint angle variability

was significantly higher on all downhill inclines, as well as at +6° and +12° inclines. (Table 14 and Figure 11).

TABLE 14. SampEn (*m*=99, *r*=4.5) of right lower limb joint angle across inclinations (n = 28)

	Hip			Knee			Ankle		
Inclination (°)	Mean	SD	p	Mean	SD	p	Mean	SD	p
-12	0.01090	0.00368	<.001*	0.02390	0.00796	<.001*	0.01760	0.00664	<.001*
-6	0.00615	0.00284	<.001*	0.01580	0.00511	<.001*	0.01180	0.00365	<.001*
-4	0.00472	0.00224	<.001*	0.01320	0.00477	<.001*	0.01030	0.00492	<.001*
-2	0.00347	0.00123	<.001*	0.00979	0.00315	<.001*	0.00894	0.00444	<.001*
0	0.00285	0.00115		0.00827	0.00313		0.00695	0.00331	
+2	0.00285	0.00099	0.635	0.00825	0.00355	0.731	0.00688	0.00363	0.364
+4	0.00322	0.00105	0.016*	0.00954	0.00299	0.004*	0.00707	0.00269	0.509
+6	0.00407	0.00174	<.001*	0.01040	0.00346	<.001*	0.00811	0.00281	<.001*
+12	0.00733	0.00332	<.001*	0.01350	0.00426	<.001*	0.01120	0.00334	<.001*

*indicates a significant difference compared to level ground walking

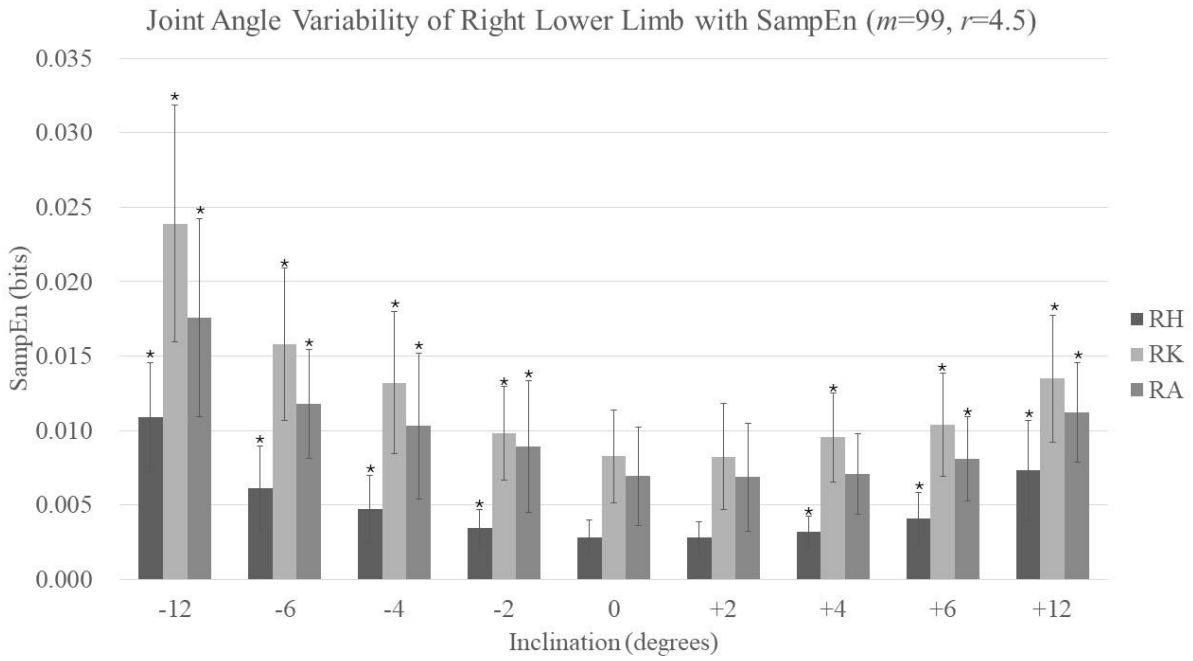

FIGURE 11. The sagittal-plane joint angle variability of the right hip (RH), right knee (RK), and right ankle (RA) computed with SampEn (*m*=99, *r*=4.5). * indicates significant differences compared to level walking.

9 DISCUSSION

This study investigated the stride-to-stride sagittal-plane joint angle variability of the lower limbs across inclinations with linear and non-linear methods. The two hypotheses of this study that sagittal-plane joint angle variability would increase as the inclination increased and the significant differences would occur at the ±12° inclines were partially supported. The following paragraphs discuss the findings of the spatiotemporal parameters and stride-to-stride sagittal-plane joint angle variability.

9.1 Spatiotemporal parameters

The alteration in spatiotemporal parameters during uphill walking in this study showed a varied trend compared to the previous studies (Kawamura et al. 1991; Leroux et al. 2002; McIntosh et al. 2006; Strutzenberger et al. 2022; Mexi et al. 2023). As the inclination increased, the participants tended to increase their cadence and decrease the stride length and step length. The reduction in stride and step length, accompanied by an increase in cadence during downhill walking, aligned with findings from the majority of previous studies (Kawamura et al. 1991; Leroux et al. 2002; Vieira et al. 2017; Dewolf et al. 2020), but contradicted McIntosh et al. (2006). The significant differences in spatiotemporal parameters were only observed at the steepest inclination during uphill walking. In deviation from our hypothesis, the significant changes presented at steepest and lower inclinations during downhill walking. This implies that downhill walking may exert a greater influence on biomechanics compared to uphill walking.

Lu et al. (2023) demonstrated that the gait stability ratio, a ratio of cadence to speed, increased during uphill walking compared to level walking, indicating a more challenging task for balance. Since the increased cadence at constant speed was observed in both uphill and downhill conditions in this study, this indicates that sloped walking is biomechanically more imbalanced than level walking. A more conservative strategy might be adopted in response to the instability and fear of falling (Maki. 1997; Scaglioni-Solano and Aragón-Vargas. 2015). As the movement strategy aims to descend the CoM smoothly and manage the shock absorption during downhill walking (Leroux et al. 2002; McIntosh et al. 2006; Dewolf et al. 2020), the participants in this study might have increased their cadence and decreased their stride length to minimize CoM vertical displacement. As a result of constant walking speed across all inclinations, the stride time and step time decreased in response to increased cadence. Furthermore, the proportion of

the stance phase in the gait cycle decreased in all downhill conditions, which might be correlated with the lower demand for propulsive force generation (Kuster et al. 1995).

In contrast to this study, some previous evidence presented a decreased cadence (Kawamura et al. 1991; Redfern and DiPasquale. 1997; McIntosh et al. 2006; Strutzenberger et al. 2022; Mexi et al. 2023) and an increased step length (Leroux et al. 2002; McIntosh et al. 2006; Strutzenberger et al. 2022; Mexi et al. 2023) with increasing positive inclination. Several possible explanations exist for the variations in gait parameters observed in different studies. First is the walking speed. Both McIntosh et al. (2006) and Kawamura et al. (1991) allowed their participants to walk at an unfixed self-selected speed. McIntosh et al. reported an increasing trend in walking speed from a 0° to a 10° upslope, whereas Kawamura et al. observed a significant decrease in speed on a 12° upslope. This inconsistency in findings might be explained by the limited length of the walking path with which the observed behavior could be derived from the regular gait pattern (McIntosh et al., 2006). Leroux et al. (2002) reported constant walking speeds ranging from 0.76 to 1.34 m/s from 0% to 10% slopes, while treadmill walking at much slower speeds may fail to reproduce the step length, step time, and cadence of ramp walking (Item-Glatthorn et al. 2016). Still, the walking speed in this study may not be an optimal representation of regular walking since it was higher than the other treadmill walking studies (Strutzenberger et al. 2022; Mexi et al. 2023). The study using a self-paced treadmill observed that the average speed significantly decreased at 10° uphill compared to level walking (Kimel-Naor et al. 2017). The participants in this study might favor increasing cadence over stride length to maintain the walking speed. In this way, they could involve fewer changes in lower limb joint moments for speed management (Ardestani et al. 2016). Accordingly, differences in gait parameter adjustments may be attributed to variations in instrumentation and protocols. Also, the gait pattern during uphill walking is likely more susceptible to these factors.

9.2 Joint angle variability

This is the first study to investigate the stride-to-stride lower limb joint angle variability on the sagittal plane during both uphill and downhill walking. Our hypothesis for the lower limb sagittal-plane joint angle variability was partially accepted. Both the linear method and the SampEn (m=99) showed that the lower limb sagittal-plane joint angle variability significantly increased during walking at +12°, -12°, and other lower inclines compared to level walking. However, with SampEn (m=2), the hypothesis regarding the lower limb sagittal-plane joint

angle variability was verified only in downhill conditions. Furthermore, SampEn (m=2) showed a U-shape trend of the lower limb sagittal-plane joint angle variability from 0° to +12°, whose lowest value existed between inclines of +2° to +4°. Regardless of the mathematic methods and walking conditions, the knee sagittal-plane joint angle variability was the highest among the lower limb joints.

This study presented that the amount of lower limb sagittal-plane joint angle variability increased as the inclination increased. Sarvestan et al. (2021) observed significant changes in sagittal-plane joint angle variability primarily during the mid to terminal stance phases during uphill walking. In this study, the components at each percentage of the gait cycle were averaged to present the average joint angle variability throughout the stride. Despite the modifications in mathematics, the results in this study were consistent with Sarvestan et al. This suggests that, while the most pronounced differences are localized in a certain range of the gait cycle, the overall impact of walking on a slope, as compared to level ground, substantially affects joint behavior throughout the cycle. In general, the trend of increasing variability of the lower limb joint angles during downhill walking and steeper uphill walking was consistent with the observations regarding the gait parameters variability on uneven surfaces (Alkjær et al. 2012; Blair et al. 2018; Sarvestan et al. 2021; Ippersiel et al. 2022) and suggested that a more flexible sensorimotor strategy was adopted among healthy adults (Stergiou. 2004; Blair et al. 2018; Ippersiel et al. 2022; Kweon et al. 2022; Mohr et al. 2023). Several factors have been assumed to be correlated with increased variability of gait parameters, including movement economics (Mohr et al. 2023), anticipatory strategy (Blair et al. 2018), impacts at ground contacts, movement speed, and demand of coordination (Estep et al. 2018). These aspects differ between sloped walking and level walking, thus potentially influencing variability.

Wenzel et al. (2023) presented that walking on uneven surfaces required higher production of lower limb power, which was achieved majorly by the hip and knee. During sloped walking, the alteration in power demands is associated with increased lower limb muscle activity (Lay et al. 2007; Franz and Kram. 2012). Specifically, the muscle activity of the hip, knee, and ankle extensors increased with power generation, particularly in the hip and ankle, which showed increased activity during uphill walking (Lay et al. 2007; Franz and Kram. 2012). Lay et al. (2007) observed that, despite the remaining knee extensor moment during uphill walking, the muscle activity of the knee extensors increased, which was considered to counteract the knee flexor moment contributed by the biarticular hip extensors (Lay et al. 2007). Correspondingly,

Franz and Kram (2012) reported the increased activity of the medial gastrocnemius, a biarticular muscle across the knee and ankle, during uphill walking. In other words, the knee is also subject to the influence of the motor strategy of the hip and ankle. This could potentially explain why the knee sagittal-plane joint angle variability was highest among lower limb joints and across all slopes. During downhill walking, the activity of the knee extensors increases with the increased power absorption at the knee (Franz and Kram. 2012). The mechanical efficiency of muscle power output is determined by the coordination pattern of muscles (Wakeling et al. 2010; Blake and Wakeling. 2015). The larger magnitude of muscle activation and the coordination pattern during sloped walking may be more complicated to the neuromuscular system and might thus alter the lower limb sagittal-plane joint angle variability.

The other possible explanation for the increased sagittal-plane joint angle variability may be the weakened balance during sloped walking. Gottschall et al. (2011) observed an increase in the base of support, a common reaction to imbalance conditions, during downhill and uphill walking. Scaglioni-Solano and Aragón-Vargas. (2015) reported that the smoothness of the pelvis movement in the anterioposterior and mediolateral direction was reduced during sloped walking, which was considered to impair balance control. As lower limbs play an important role in smoothing the trajectory of the pelvis (Leroux et al. 2002), increased lower limb kinematic variability may allow the sensorimotor system to generate flexible strategies to enhance the smoothness of pelvis trajectory and regain balance (Stergiou. 2004; Scaglioni-Solano and Aragón-Vargas. 2015). Qiao et al. (2018) studied the balance perturbation of the optical flow on the step-to-step adjustments in gait parameters of young and older adults. They concluded that the knee sagittal-plane joint angle variability was positively correlated with the step length variability, and the hip coronal-plane joint angle variability was correlated with the step width variability (Qiao et al. 2018). According to Sturk et al. (2019), step length variability increased when walking on uneven surfaces. This adjustment in foot placement under balance perturbations may interact with the lower limb kinematics and potentially increase variability in lower limb joint angles during sloped walking.

The structure of the sagittal-plane joint angle variability showed partially different results from the amount of variability. With SampEn, with a vector length of two data points, the lower limb sagittal-plane joint angle variability still increased with the walking surface becoming more declined. On the other hand, the sagittal-plane joint angle variability of the hip and knee in lower upward inclinations significantly decreased and increased at +12 degrees compared to

level walking. Correspondingly, Vieira et al. (2017) demonstrated that the complexity of trunk velocity, as measured by SampEn (m=2, r=0.2), decreased linearly from the 10% (5.7°) downhill to the 10% uphill conditions. Conclusively, the structure of the sagittal-plane joint angle variability was aligned with the amount of the sagittal-plane joint angle variability during downhill walking regardless of the steepness of the incline. On the opposite, the structure of the sagittal-plane joint angle variability was composed of less mild fluctuations during walking at lower positive inclines, which indicated less complexity in the time series. Moreover, the larger perturbation from the higher inclines may alter the mechanism of adjusting this complexity of joint angle patterns. The SampEn with a vector length of 99 showed a similar trend as the results of the linear method. It may indicate that the probability of one random stride movement pattern occurring in a time series is similar to the amount of variability.

The three methods applied in this study have their strengths and weaknesses and each of them approaches the movement variability from different perspectives. Exploring variability with standard deviation offers a straightforward interpretation and provides a more detailed view of stride-to-stride joint angle variability. However, this method is also more susceptible to the influence of outliers. If the joint angle at a specific time point in one gait cycle is considerably higher for one participant than for other participants at the same time point, the standard deviation will be biased. SampEn, with a vector length of two, measures the predictability of patterns consisting of two consecutive joint angle values in a time series. Specifically, the pattern from 1-2% of the first gait cycle is compared not only to the same interval in subsequent gait cycles but also across different intervals such as 3-4% and 4-5%, and even across cycle boundaries, like from 100% of the 1st cycle to 1% of the 2nd cycle. This approach, with its relatively short vector length, tends to highlight the complexity of the joint angle pattern over the entire series, capturing mild fluctuations within a gait cycle. Moreover, when humans walk on inclined surfaces, changes in kinematics can significantly alter movement patterns and range of motions, potentially leading to variations in SampEn values. This suggests that different walking conditions, such as inclined versus level surfaces, might influence the predictability and complexity of joint movements as captured by SampEn. When the vector length increases from 2 to 99, each vector effectively approximates a complete gait cycle. Based on this assumption, the SampEn measures the probability that a gait cycle pattern repeats within the time series. However, when comparing vectors with a large number of components, a higher tolerance must be set to allow for pattern matching. As any variance within this relatively large tolerance level is not recognized as a new pattern, the SampEn output value (m=99) indicates

high regularity across all conditions and potentially masks the slight differences. The optimal choices of sample entropy parameters for joint angle in gait analysis require more future investigation.

9.3 Limitations

A previous study reported that treadmill walking reduced the variability compared to overground walking (Dingwell et al. 2001). It is reasonable as treadmill walking generally restricts the variation of walking speed and direction of progression. Specifically, the spatiotemporal parameters, force profile, and energy consumption are different between treadmill and overground walking, and the fear of falling or losing control may lead to a more conservative gait pattern (Vickery-Howe et al. 2023). These factors may also induce a distinct sensorimotor strategy, and thus affect the variability. Therefore, caution should be exercised when trying to directly apply or compare the results of this study to overground walking situations. Despite the importance of studying overground walking, it may be methodologically more challenging to obtain enough data points for entropy analysis. Another concern about using a treadmill protocol is the mechanical noise which may influence the joint angle fluctuations. While applying a filter allows a smoother and less noisy joint angle curve, it diminishes the mild biological information within it at the same time. Hence, a study carried out on a ramp rather than on a treadmill is required to better understand how humans react to inclinations.

The average walking speed of the participants in this study was higher than in the previous studies. Zoffoli et al. (2017) reported that a faster walking speed which was close to the transition to running resulted in a higher kinematic variability. Beauchet et al. (2009) observed a decreased stride time variability at a lower walking speed. Since the populations with health conditions or older age prefer slower walking speeds, the observed sensorimotor adjustment in response to slopes may differ from this study. They are also more likely to fall when encountering balance perturbations. Accordingly, investigating the joint angle variability during sloped walking at a slower speed and with different populations is important to know its relationship with fall risks. Furthermore, the walking speed was selected based on the subjective perception at level walking. Some participants might not walk at the most efficient speed for their energy system. The differences among participants may lead to a larger deviation in biomechanics and physiology during steep uphill and downhill walking. Applying the same

speed as level walking during sloped walking may also contradict the natural strategy (Perrey and Fabre. 2008).

The order of the inclines was not completely randomized and the rest periods between the trials were short. Dos Anjos et al. (2023) concluded that the trunk acceleration variability was significantly increased immediately after a fatigue protocol and returned to its baseline after resting for 4 minutes. The steepest uphill and downhill walking were arranged as the last two measured trials and there was no monitoring of any indicators of fatigue during the measurement. Thus, this study can hardly exclude the potential effect of fatigue on the variability during walking on the steepest slopes despite the short walking duration for the steepest inclinations.

The lower limb sagittal-plane joint angle variability results showed slight differences between the left and right sides. The discrepancy in participant numbers might be the reason for it when considering statistics. During the measurement, the participants walked on the side of the treadmill closer to the left MoCap cameras. This positioning resulted in a greater chance of occlusion of markers on the left lower limb. As the duration of the marker occlusion increased, the precision of the gap-filling algorithm to estimate missing marker positions decreased (Howarth and Callaghan. 2010). This diminished precision likely introduced trajectories with computational artifacts, subsequently leading to a reduced dataset for the analysis of the left side. Another methodology consideration under caution is the gait event detection algorithm. The hallux markers were used instead of the toe markers for the FO detection. Although Bruening and Ridge (2014) recommended using the hallux marker to enhance the accuracy of the toe off detection, it hasn’t been verified during sloped walking. Also, the results showed that the errors existed between the timings identified through the visual inspection and the automatic algorithm. When the joint angle was time normalized to the gait cycle, the errors in timing implied a potential distortion in the shape of the joint angle curve. The differences between the compared patterns could arise from this disadvantage in the method.

In this study, only the sagittal-plane joint angle variability was examined, while the previous research presented that the adaptation of the joint angle variability occurred on other movement planes as well (Sarvestan et al. 2021). Since the kinematics of human gait do not take place in a single direction, future studies should include the frontal and horizontal plane movement to draw a thorough conclusion on the impacts of slopes on the joint angle variability.

10 CONCLUSION

In this study, the adjustments in spatiotemporal parameters during uphill and downhill walking were partially consistent with the findings of previous studies, suggesting that they might be affected by factors like walking speed, surfaces, and preferred strategies. The inclinations had significant effects on the amount and the structure of the hip, knee, and ankle sagittal-plane joint angle variability during walking. The amount of the sagittal-plane joint angle variability significantly increased as the treadmill became more inclined or declined. The structure of the sagittal-plane joint angle variability walking showed a similar trend as the amount of variability during downhill, while the structure of the sagittal-plane hip and knee joint angle variability of uphill walking significantly decreased at lower positive inclinations and increased at higher inclinations. The possible mechanisms behind the adaptation included greater muscular activation, distinct power demands, and larger balance perturbations during sloped walking. The assumption about challenges in balance could be supported by the changes in the spatiotemporal parameters which indicated the adoption of a more conservative gait strategy during downhill walking and steep uphill walking. Future research combining other biomechanics measurements is required to explore the determinants of the lower limb joint angle variability.

Although this study did not quantify the optimized range for the sagittal-plane joint angle variability, it provided a perspective on how sensorimotor strategy reacted to various inclinations when walking on the treadmill. Moreover, the results suggested that the amount and the structure of the lower limb sagittal-plane joint angle variability did not respond to the perturbation identically. The structure of the sagittal-plane joint angle variability computed via sample entropy should be interpreted carefully since the chosen parameters, such as vector length and tolerance level, directly determine the way to compare patterns. While the commonly adopted vector length (m=2) captures the mild variance within the time series and allows the comparison to previous studies, it yields obstacles to interpreting the biological meaning. This is the first study to apply a vector length of 99 that enables the comparison between the joint angle curve of a gait cycle to another. However, due to the mathematical constraints, a relatively high tolerance level is required to have a matched pattern in the time series and produce consistent results. It is still a question of whether the low threshold is suitable or meaningful enough for investigating stride-to-stride joint angle variability.

To widely apply the joint angle variability during sloped walking in practice, studies targeting populations with higher fall risks, such as older adults or people with impaired neuromuscular control are needed. Furthermore, treadmill walking is biomechanically different from overground walking. The protocols that allow long recording lengths to analyze the amount and the structure of joint angle variability will benefit our understanding of it.

In conclusion, healthy adults altered their sensorimotor strategy during sloped walking. The increase in movement variability suggested that they used a more flexible and more adaptative sensorimotor strategy during sloped walking compared to level walking. In addition, the adjustments were task-specific as they differed between positive, negative, lower and higher inclinations.

REFERENCES

Alexander, N., & Schwameder, H. (2023). A forefoot strike pattern during 18° uphill walking leads to the greater ankle joint and plantar flexor loading. Gait & posture, 103, 44–49. https://doi.org/10.1016/j.gaitpost.2023.04.011

Anaconda Inc. (2023). Anaconda Navigator (Version 2.5.0) [Computer Software]. Retrieved from https://www.anaconda.com

Anang, N., Jailani, R., Tahir, N., Manaf, H., & Mustafah, N. (2016). Analysis of kinematic gait parameters in chronic stroke survivors. 57–62. https://doi.org/10.1109/ISCAIE.2016.7575037

Ardestani, M. M., Ferrigno, C., Moazen, M., & Wimmer, M. A. (2016). From normal to fast walking: Impact of cadence and stride length on lower extremity joint moments. Gait & posture, 46, 118–125. https://doi.org/10.1016/j.gaitpost.2016.02.005

Baida, S. R., Gore, S. J., Franklyn-Miller, A. D., & Moran, K. A. (2018). Does the amount of lower extremity movement variability differ between injured and uninjured populations? A systematic review. Scandinavian journal of medicine & science in sports, 28(4), 1320–1338. https://doi.org/10.1111/sms.13036

Barré, A., & Armand, S. (2014). Biomechanical ToolKit: Open-source framework to visualize and process biomechanical data. Computer methods and programs in biomedicine, 114(1), 80–87. https://doi.org/10.1016/j.cmpb.2014.01.012

Bauer, J. P., Sienko, S., & Davids, J. R. (2022). Idiopathic Toe Walking: An Update on Natural History, Diagnosis, and Treatment. The Journal of the American Academy of Orthopaedic Surgeons, 30(22), e1419–e1430. https://doi.org/10.5435/JAAOS-D-22-00419

Beauchet, O., Annweiler, C., Lecordroch, Y., Allali, G., Dubost, V., Herrmann, F. R., & Kressig, R. W. (2009). Walking speed-related changes in stride time variability: effects of decreased speed. Journal of neuroengineering and rehabilitation, 6, 32. https://doi.org/10.1186/1743-0003-6-32

Blair, S., Lake, M. J., Ding, R., & Sterzing, T. (2018). Magnitude and variability of gait characteristics when walking on an irregular surface at different speeds. Human movement science, 59, 112–120. https://doi.org/10.1016/j.humov.2018.04.003

Blake, O. M., & Wakeling, J. M. (2015). Muscle coordination limits efficiency and power output of human limb movement under a wide range of mechanical demands. Journal of neurophysiology, 114(6), 3283–3295. https://doi.org/10.1152/jn.00765.2015

Blyton, S. J., Snodgrass, S. J., Pizzari, T., Birse, S. M., Likens, A. D., & Edwards, S. (2023). The impact of previous musculoskeletal injury on running gait variability: A systematic review. Gait & posture, 101, 124–133. https://doi.org/10.1016/j.gaitpost.2023.01.018

Boucher, P., Teasdale, N., Courtemanche, R., Bard, C., & Fleury, M. (1995). Postural stability in diabetic polyneuropathy. Diabetes care, 18(5), 638–645. https://doi.org/10.2337/diacare.18.5.638

Brach, J. S., Berlin, J. E., VanSwearingen, J. M., Newman, A. B., & Studenski, S. A. (2005). Too much or too little step width variability is associated with a fall history in older persons who walk at or near normal gait speed. Journal of NeuroEngineering and Rehabilitation, 2, 21. https://doi.org/10.1186/1743-0003-2-21

Bruening, D. A., Cooney, K. M., & Buczek, F. L. (2012). Analysis of a kinetic multi-segment foot model part II: kinetics and clinical implications. Gait & posture, 35(4), 535–540. https://doi.org/10.1016/j.gaitpost.2011.11.012

Bruening, D. A., & Ridge, S. T. (2014). Automated event detection algorithms in pathological gait. Gait & posture, 39(1), 472–477. https://doi.org/10.1016/j.gaitpost.2013.08.023

Bueno, G. A. S., Gervásio, F. M., Ribeiro, D. M., Martins, A. C., Lemos, T. V., & de Menezes, R. L. (2019). Fear of Falling Contributing to Cautious Gait Pattern in Women Exposed to a Fictional Disturbing Factor: A Non-randomized Clinical Trial. Frontiers in neurology, 10, 283. https://doi.org/10.3389/fneur.2019.00283

Bruening, D. A., & Ridge, S. T. (2014). Automated event detection algorithms in pathological gait. Gait & Posture, 39(1), 472–477. https://doi.org/10.1016/j.gaitpost.2013.08.023

Calais-Germain, B. (2007). Anatomy of movement (Rev. ed.). Eastland Press.

Camargo, J., Ramanathan, A., Csomay-Shanklin, N., & Young, A. (2020). Automated gap-filling for marker-based biomechanical motion capture data. Computer methods in biomechanics and biomedical engineering, 23(15), 1180–1189. https://doi.org/10.1080/10255842.2020.1789971

Caron-Laramée, A., Walha, R., Boissy, P., Gaudreault, N., Zelovic, N., & Lebel, K. (2023). Comparison of Three Motion Capture-Based Algorithms for Spatiotemporal Gait Characteristics: How Do Algorithms Affect Accuracy and Precision of Clinical Outcomes? Sensors (Basel, Switzerland), 23(4), 2209. https://doi.org/10.3390/s23042209

Georgoulis, A. D., Moraiti, C., Ristanis, S., & Stergiou, N. (2006). A Novel Approach to Measure Variability in the Anterior Cruciate Ligament Deficient Knee During Walking:

The Use of the Approximate Entropy in Orthopaedics. Journal of Clinical Monitoring and Computing, 20(1), 11–18. https://doi.org/10.1007/s10877-006-1032-7

Dewolf, A. H., Mesquita, R. M., & Willems, P. A. (2020). Intra-limb and muscular coordination during walking on slopes. European Journal of Applied Physiology, 120(8), 1841–1854. https://doi.org/10.1007/s00421-020-04415-4

Dingwell, J. B., & Cusumano, J. P. (2000). Nonlinear time series analysis of normal and pathological human walking. Chaos: An Interdisciplinary Journal of Nonlinear Science, 10(4), 848–863. https://doi.org/10.1063/1.1324008

Dingwell, J. B., Cusumano, J. P., Cavanagh, P. R., & Sternad, D. (2001). Local dynamic stability versus kinematic variability of continuous overground and treadmill walking. Journal of biomechanical engineering, 123(1), 27–32. https://doi.org/10.1115/1.1336798

Dixon, P. C., Böhm, H., & Döderlein, L. (2012). Ankle and midfoot kinetics during normal gait: a multi-segment approach. Journal of biomechanics, 45(6), 1011–1016. https://doi.org/10.1016/j.jbiomech.2012.01.001

Dos Anjos, L., Rodrigues, F., Scataglini, S., Baptista, R. R., Lobo da Costa, P., & Vieira, M. F. (2023). Trunk variability and local dynamic stability during gait after generalized fatigue induced by incremental exercise test in young women in different phases of the menstrual cycle. PeerJ, 11, e16223. https://doi.org/10.7717/peerj.16223

Erdemir, A., Hamel, A. J., Fauth, A. R., Piazza, S. J., & Sharkey, N. A. (2004). Dynamic loading of the plantar aponeurosis in walking. The Journal of bone and joint surgery. American volume, 86(3), 546–552. https://doi.org/10.2106/00004623-200403000-00013

Fallahtafti, F., Salamifar, Z., Hassan, M., Rahman, H., Pipinos, I., & Myers, S. A. (2022). Joint Angle Variability Is Altered in Patients with Peripheral Artery Disease after Six Months of Exercise Intervention. Entropy, 24(10), Article 10. https://doi.org/10.3390/e24101422

Fallahtafti, F., Wurdeman, S. R., & Yentes, J. M. (2021). Sampling rate influences the regularity analysis of temporal domain measures of walking more than spatial domain measures. Gait & posture, 88, 216–220. https://doi.org/10.1016/j.gaitpost.2021.05.031

Fetto J. F. (2019). A Dynamic Model of Hip Joint Biomechanics: The Contribution of Soft Tissues. Advances in orthopedics, 2019, 5804642. https://doi.org/10.1155/2019/5804642

Franklin, S., Grey, M. J., Heneghan, N., Bowen, L., & Li, F. X. (2015). Barefoot vs common footwear: A systematic review of the kinematic, kinetic and muscle activity differences

during walking. Gait & posture, 42(3), 230–239. https://doi.org/10.1016/j.gaitpost.2015.05.019

Franz, J. R., & Kram, R. (2012). The effects of grade and speed on leg muscle activations during walking. Gait & posture, 35(1), 143–147. https://doi.org/10.1016/j.gaitpost.2011.08.025

Fraser, J. J., Feger, M. A., & Hertel, J. (2016). MIDFOOT AND FOREFOOT INVOLVEMENT IN LATERAL ANKLE SPRAINS AND CHRONIC ANKLE INSTABILITY. PART 1: ANATOMY AND BIOMECHANICS. International journal of sports physical therapy, 11(6), 992–1005.

Ghoussayni, S., Stevens, C., Durham, S., & Ewins, D. (2004). Assessment and validation of a simple automated method for the detection of gait events and intervals. Gait & Posture, 20(3), 266–272. https://doi.org/10.1016/j.gaitpost.2003.10.001

Gomes, D., Guimarães, V., & Silva, J. (2021). A Fully-Automatic Gap Filling Approach for Motion Capture Trajectories. Applied Sciences, 11(21), Article 21. https://doi.org/10.3390/app11219847

Gottschall, J. S., Okorokov, D. Y., Okita, N., & Stern, K. A. (2011). Walking strategies during the transition between level and hill surfaces. Journal of applied biomechanics, 27(4), 355–361. https://doi.org/10.1123/jab.27.4.355

Hamill, J., van Emmerik, R. E., Heiderscheit, B. C., & Li, L. (1999). A dynamical systems approach to lower extremity running injuries. Clinical biomechanics (Bristol, Avon), 14(5), 297–308. https://doi.org/10.1016/s0268-0033(98)90092-4

Hamill, J., Palmer, C., & Van Emmerik, R. E. (2012). Coordinative variability and overuse injury. Sports medicine, arthroscopy, rehabilitation, therapy & technology: SMARTT, 4(1), 45. https://doi.org/10.1186/1758-2555-4-45

Hansen, A. H., Childress, D. S., & Meier, M. R. (2002). A simple method for determination of gait events. Journal of Biomechanics, 35(1), 135–138. https://doi.org/10.1016/S0021-9290(01)00174-9

Harbourne RT, Stergiou N. Perspective movement variability and the use of nonlinear tools: principles to guide physical therapist practice. Phys Ther. 2009; 89: 267-282.

Harris, C. M., & Wolpert, D. M. (1998). Signal-dependent noise determines motor planning. Nature, 394(6695), 780–784. https://doi.org/10.1038/29528

Hausdorff, J. M., Purdon, P. L., Peng, C. K., Ladin, Z., Wei, J. Y., & Goldberger, A. L. (1996). Fractal dynamics of human gait: stability of long-range correlations in stride interval

fluctuations. Journal of applied physiology (Bethesda, Md.: 1985), 80(5), 1448–1457. https://doi.org/10.1152/jappl.1996.80.5.1448

Hebenstreit, F., Leibold, A., Krinner, S., Welsch, G., Lochmann, M., & Eskofier, B. M. (2015). Effect of walking speed on gait sub phase durations. Human movement science, 43, 118–124. https://doi.org/10.1016/j.humov.2015.07.009

Hong, S.-W., Leu, T.-H., Li, J.-D., Wang, T.-M., Ho, W.-P., & Lu, T.-W. (2014). Influence of inclination angles on intra- and inter-limb load-sharing during uphill walking. Gait & Posture, 39(1), 29–34. https://doi.org/10.1016/j.gaitpost.2013.05.023

Howarth, S. J., & Callaghan, J. P. (2010). Quantitative assessment of the accuracy for three interpolation techniques in kinematic analysis of human movement. Computer methods in biomechanics and biomedical engineering, 13(6), 847–855. https://doi.org/10.1080/10255841003664701

Hreljac, A., & Marshall, R. N. (2000). Algorithms to determine event timing during normal walking using kinematic data. Journal of Biomechanics, 33(6), 783–786. https://doi.org/10.1016/S0021-9290(00)00014-2

Ippersiel, P., Shah, V., & Dixon, P. C. (2022). The impact of outdoor walking surfaces on lower-limb coordination and variability during gait in healthy adults. Gait & posture, 91, 7–13. https://doi.org/10.1016/j.gaitpost.2021.09.176

Item-Glatthorn, J. F., Casartelli, N. C., & Maffiuletti, N. A. (2016). Reproducibility of gait parameters at different surface inclinations and speeds using an instrumented treadmill system. Gait & posture, 44, 259–264. https://doi.org/10.1016/j.gaitpost.2015.12.037

The jamovi project (2023). jamovi (Version 2.3) [Computer Software]. Retrieved from https://www.jamovi.org

Kadaba, M. P., Ramakrishnan, H. K., & Wootten, M. E. (1990). Measurement of lower extremity kinematics during level walking. Journal of orthopaedic research: official publication of the Orthopaedic Research Society, 8(3), 383–392. https://doi.org/10.1002/jor.1100080310

Kawamura, K., Tokuhiro, A., & Takechi, H. (1991). Gait analysis of slope walking: A study on step length, stride width, time factors and deviation in the center of pressure. Acta Medica Okayama, 45(3), 179–184. https://doi.org/10.18926/AMO/32212

Kimel-Naor, S., Gottlieb, A., & Plotnik, M. (2017). The effect of uphill and downhill walking on gait parameters: A self-paced treadmill study. Journal of biomechanics, 60, 142–149. https://doi.org/10.1016/j.jbiomech.2017.06.030

Kingma, I., de Looze, M. P., Toussaint, H. M., Klijnsma, H. G., & Bruijnen, T. B. M. (1996). Validation of a full body 3-D dynamic linked segment model. Human Movement Science, 15(6), 833–860. https://doi.org/10.1016/S0167-9457(96)00034-6

Kuster, M., Sakurai, S., & Wood, G. A. (1995). Kinematic and kinetic comparison of downhill and level walking. Clinical biomechanics (Bristol, Avon), 10(2), 79–84. https://doi.org/10.1016/0268-0033(95)92043-l

Kweon, S. J., Harrison, K., Williams, D. S. B., 3rd, & Kwon, Y. U. (2022). Foot and Shank Coordination During Walking in Copers Compared With Patients With Chronic Ankle Instability and Controls. Orthopaedic journal of sports medicine, 10(12), 23259671221139482. https://doi.org/10.1177/23259671221139482

Lay, A. N., Hass, C. J., Richard Nichols, T., & Gregor, R. J. (2007). The effects of sloped surfaces on locomotion: an electromyographic analysis. Journal of biomechanics, 40(6), 1276–1285. https://doi.org/10.1016/j.jbiomech.2006.05.023

Leboeuf, F., Barre, A., Aminian, K., & Sangeux, M. (2023). On the accuracy of the Conventional gait Model: Distinction between marker misplacement and soft tissue artefact errors. Journal of biomechanics, 159, 111774. https://doi.org/10.1016/j.jbiomech.2023.111774

Lee, M., Noh, Y., Youm, C., Kim, S., Park, H., Noh, B., Kim, B., Choi, H., & Yoon, H. (2021). Estimating Health-Related Quality of Life Based on Demographic Characteristics, Questionnaires, Gait Ability, and Physical Fitness in Korean Elderly Adults. International journal of environmental research and public health, 18(22), 11816. https://doi.org/10.3390/ijerph182211816

Leroux, A., Fung, J., & Barbeau, H. (2002). Postural adaptation to walking on inclined surfaces: I. Normal strategies. Gait & posture, 15(1), 64–74. https://doi.org/10.1016/s0966-6362(01)00181-3

Loverro, K. L., Khuu, A., Kao, P. C., & Lewis, C. L. (2019). Kinematic variability and local dynamic stability of gait in individuals with hip pain and a history of developmental dysplasia. Gait & posture, 68, 545–554. https://doi.org/10.1016/j.gaitpost.2019.01.007

Lu, C., Al-Juaid, R., & Al-Amri, M. (2023). Gait Stability Characteristics in Able-Bodied Individuals During Self-paced Inclined Treadmill Walking: Within-Subject Repeated-Measures Study. JMIR formative research, 7, e42769. https://doi.org/10.2196/42769

Lu, S., Chen, X., Kanters, J. K., Solomon, I. C., & Chon, K. H. (2008). Automatic selection of the threshold value R for approximate entropy. IEEE transactions on bio-medical engineering, 55(8), 1966–1972. https://doi.org/10.1109/TBME.2008.919870

Maki B. E. (1997). Gait changes in older adults: predictors of falls or indicators of fear. Journal of the American Geriatrics Society, 45(3), 313–320. https://doi.org/10.1111/j.1532-5415.1997.tb00946.x

Marmelat, V., Duncan, A., & Meltz, S. (2019). Effect of sampling frequency on fractal fluctuations during treadmill walking. PloS one, 14(11), e0218908. https://doi.org/10.1371/journal.pone.0218908

MathWorks. (2023). MATLAB (Version 2023a) [Computer software]. Retrieved from https://www.mathworks.com

McCamley, J. D., Denton, W., Arnold, A., Raffalt, P. C., & Yentes, J. M. (2018). On the calculation of sample entropy using continuous and discrete human gait data. Entropy (Basel, Switzerland), 20(10), 764. https://doi.org/10.3390/e20100764

McIntosh, A. S., Beatty, K. T., Dwan, L. N., & Vickers, D. R. (2006). Gait dynamics on an inclined walkway. Journal of Biomechanics, 39(13), 2491–2502. https://doi.org/10.1016/j.jbiomech.2005.07.025

Mexi, A., Kafetzakis, I., Korontzi, M., Karagiannakis, D., Kalatzis, P., & Mandalidis, D. (2023). Effects of Load Carriage on Postural Control and Spatiotemporal Gait Parameters during Level and Uphill Walking. Sensors (Basel, Switzerland), 23(2), 609. https://doi.org/10.3390/s23020609

Mohammadzadeh Gonabadi, A., Cesar, G. M., Buster, T. W., & Burnfield, J. M. (2022). Effect of gap-filling technique and gap location on linear and nonlinear calculations of motion during locomotor activities. Gait & Posture, 94, 85–92. https://doi.org/10.1016/j.gaitpost.2022.02.025

Mohr, M., Peer, L., De Michiel, A., van Andel, S., & Federolf, P. (2023). Whole-body kinematic adaptations to running on an unstable, irregular, and compliant surface. Sports biomechanics, 1–15. Advance online publication. https://doi.org/10.1080/14763141.2023.2222022

Muybridge, E. (1887). Animal locomotion (Vol. 534). Da Capo Press.

Nair, S. P., Gibbs, S., Arnold, G., Abboud, R., & Wang, W. (2010). A method to calculate the centre of the ankle joint: a comparison with the Vicon Plug-in-Gait model. Clinical biomechanics (Bristol, Avon), 25(6), 582–587. https://doi.org/10.1016/j.clinbiomech.2010.03.004

Newell, K. M. & Corcos, D. M. (1993). Variability and motor control. Human Kinetics.

Núñez-Trull, A., Álvarez-Medina, J., Jaén-Carrillo, D., Rubio-Peirotén, A., Roche-Seruendo, L. E., & Gómez-Trullén, E. M. (2023). Influence of walking speed on gait

spatiotemporal parameters and the functional rockers of the foot in healthy adults. Medical engineering & physics, 117, 104002. https://doi.org/10.1016/j.medengphy.2023.104002

Pantall, A., Gregor, R. J., & Prilutsky, B. I. (2012). Stance and swing phase detection during level and slope walking in the cat: Effects of slope, injury, subject and kinematic detection method. Journal of Biomechanics, 45(8), 1529–1533. https://doi.org/10.1016/j.jbiomech.2012.03.013

Perrey, S., & Fabre, N. (2008). Exertion during uphill, level and downhill walking with and without hiking poles. Journal of sports science & medicine, 7(1), 32–38.

Pijnappels, M., Bobbert, M. F., & van Dieën, J. H. (2001). Changes in walking pattern caused by the possibility of a tripping reaction. Gait & posture, 14(1), 11–18. https://doi.org/10.1016/s0966-6362(01)00110-2

Pincus S. M. (1991). Approximate entropy as a measure of system complexity. Proceedings of the National Academy of Sciences of the United States of America, 88(6), 2297–2301. https://doi.org/10.1073/pnas.88.6.2297

Pincus, S. M., & Goldberger, A. L. (1994). Physiological time-series analysis: what does regularity quantify?. The American journal of physiology, 266(4 Pt 2), H1643–H1656. https://doi.org/10.1152/ajpheart.1994.266.4.H1643

Pothrat, C., Authier, G., Viehweger, E., Berton, E., & Rao, G. (2015). One- and multi-segment foot models lead to opposite results on ankle joint kinematics during gait: Implications for clinical assessment. Clinical biomechanics (Bristol, Avon), 30(5), 493–499. https://doi.org/10.1016/j.clinbiomech.2015.03.004

Prentice, S. D., Hasler, E. N., Groves, J. J., & Frank, J. S. (2004). Locomotor adaptations for changes in the slope of the walking surface. Gait & posture, 20(3), 255–265. https://doi.org/10.1016/j.gaitpost.2003.09.006

Qiao, M., Feld, J. A., & Franz, J. R. (2018). Aging effects on leg joint variability during walking with balance perturbations. Gait & Posture, 62, 27–33. https://doi.org/10.1016/j.gaitpost.2018.02.020

Raffalt, P. C., McCamley, J., Denton, W., & Yentes, J. M. (2019). Sampling frequency influences sample entropy of kinematics during walking. Medical & biological engineering & computing, 57(4), 759–764. https://doi.org/10.1007/s11517-018-1920-2

Redfern, J., DiPasquale, J. (1997). Biomechanics of descending ramps. Gait & posture, 6(2), 119-125. https://doi.org/10.1016/S0966-6362(97)01117-X.

Richman, J. S., & Moorman, J. R. (2000). Physiological time-series analysis using approximate entropy and sample entropy. American journal of physiology. Heart and circulatory physiology, 278(6), H2039–H2049. https://doi.org/10.1152/ajpheart.2000.278.6.H2039

Roberts, M., Mongeon, D., & Prince, F. (2017). Biomechanical parameters for gait analysis: A systematic review of healthy human gait. Physical Therapy and Rehabilitation, 4(1), Article 1.

Robertson, D., Caldwell, G., Hamill, J., Kamen, G., & Whittlesey, S. (2013). Research Methods in Biomechanics (2nd ed.). Human Kinetics

Rosenblatt, N. J., Bauer, A., CPO, Rotter, D., CPO, & Grabiner, M. D. (2014a). Active dorsiflexing prostheses may reduce trip-related fall risk in people with transtibial amputation. Journal of rehabilitation research and development, 51(8), 1229–1242. https://doi.org/10.1682/JRRD.2014.01.0031

Rosenblatt, N. J., Hurt, C. P., Latash, M. L., & Grabiner, M. D. (2014b). An apparent contradiction: increasing variability to achieve greater precision?. Experimental brain research, 232(2), 403–413. https://doi.org/10.1007/s00221-013-3748-1

Sarvestan, J., Ataabadi, P. A., Yazdanbakhsh, F., Abbasi, S., Abbasi, A., & Svoboda, Z. (2021). Lower limb joint angles and their variability during uphill walking. Gait & Posture, 90, 434–440. https://doi.org/10.1016/j.gaitpost.2021.09.195

Scaglioni-Solano, P., & Aragón-Vargas, L. F. (2015). Age-related differences when walking downhill on different sloped terrains. Gait & posture, 41(1), 153–158. https://doi.org/10.1016/j.gaitpost.2014.09.022

Sheehan, R. C., & Gottschall, J. S. (2012). At similar angles, slope walking has a greater fall risk than stair walking. Applied Ergonomics, 43(3), 473–478. https://doi.org/10.1016/j.apergo.2011.07.004

Spyder Developers. (2023) Spyder IDE. (Version 5.4.5) [Computer Software]. Retrieved from https://www.spyder-ide.org/

Stergiou, N. (2004). Innovative analyses of human movement. Champaign, IL: Human Kinetics.

Stimpson, K. H., Heitkamp, L. N., Embry, A. E., & Dean, J. C. (2019). Post-stroke deficits in the step-by-step control of paretic step width. Gait & posture, 70, 136–140. https://doi.org/10.1016/j.gaitpost.2019.03.003

Strutzenberger, G., Leutgeb, L., Claußen, L., & Schwameder, H. (2022). Gait on slopes: Differences in temporo-spatial, kinematic and kinetic gait parameters between walking on a ramp and on a treadmill. Gait & posture, 91, 73–78. https://doi.org/10.1016/j.gaitpost.2021.09.196

Sturk, J. A., Lemaire, E. D., Sinitski, E. H., Dudek, N. L., Besemann, M., Hebert, J. S., & Baddour, N. (2019). Maintaining stable transfemoral amputee gait on level, sloped and simulated uneven conditions in a virtual environment. Disability and rehabilitation. Assistive technology, 14(3), 226–235. https://doi.org/10.1080/17483107.2017.1420250

Tokuda, K., Anan, M., Takahashi, M., Sawada, T., Tanimoto, K., Kito, N., & Shinkoda, K. (2018). Biomechanical mechanism of lateral trunk lean gait for knee osteoarthritis patients. Journal of biomechanics, 66, 10–17. https://doi.org/10.1016/j.jbiomech.2017.10.016

Terada, M., Bowker, S., Thomas, A. C., Pietrosimone, B., Hiller, C. E., Rice, M. S., & Gribble, P. A. (2015). Alterations in stride-to-stride variability during walking in individuals with chronic ankle instability. Human Movement Science, 40, 154–162. https://doi.org/10.1016/j.humov.2014.12.004

Tulchin, K., Orendurff, M., Adolfsen, S., & Karol, L. (2009). The effects of walking speed on multisegment foot kinematics in adults. Journal of applied biomechanics, 25(4), 377–386. https://doi.org/10.1123/jab.25.4.377

Tunca, C., Pehlivan, N., Ak, N., Arnrich, B., Salur, G., & Ersoy, C. (2017). Inertial Sensor-Based Robust Gait Analysis in Non-Hospital Settings for Neurological Disorders. Sensors (Basel, Switzerland), 17(4), 825. https://doi.org/10.3390/s17040825

Vallat, R. (2021). Antropy. GitHub repository. https://github.com/raphaelvallat/antropy

Vickery-Howe, D. M., Bonanno, D. R., Dascombe, B. J., Drain, J. R., Clarke, A. C., Hoolihan, B., Willy, R. W., & Middleton, K. J. (2023). Physiological, perceptual, and biomechanical differences between treadmill and overground walking in healthy adults: A systematic review and meta-analysis. Journal of sports sciences, 41(23), 2088–2120. https://doi.org/10.1080/02640414.2024.2312481

Vicon Motion Systems Ltd. Vicon Nexus User Guide. Available online: https://help.vicon.com/space/Nexus216

Vieira, M. F., Rodrigues, F. B., de Sá E Souza, G. S., Magnani, R. M., Lehnen, G. C., Campos, N. G., & Andrade, A. O. (2017). Gait stability, variability and complexity on inclined surfaces. Journal of biomechanics, 54, 73–79. https://doi.org/10.1016/j.jbiomech.2017.01.045

Visscher, R. M. S., Freslier, M., Moissenet, F., Sansgiri, S., Singh, N. B., Viehweger, E., Taylor, W. R., & Brunner, R. (2021). Impact of the Marker Set Configuration on the Accuracy of Gait Event Detection in Healthy and Pathological Subjects. Frontiers in human neuroscience, 15, 720699. https://doi.org/10.3389/fnhum.2021.720699

Wakeling, J. M., Blake, O. M., & Chan, H. K. (2010). Muscle coordination is key to the power output and mechanical efficiency of limb movements. The Journal of experimental biology, 213(3), 487–492. https://doi.org/10.1242/jeb.036236

Wen, C., Cates, H. E., & Zhang, S. (2019). Is knee biomechanics different in uphill walking on different slopes for older adults with total knee replacement? Journal of Biomechanics, 89, 40–47. https://doi.org/10.1016/j.jbiomech.2019.04.006

Wenzel, T. A., Hunt, N. L., Holcomb, A. E., Fitzpatrick, C. K., & Brown, T. N. (2023). Surface, but Not Age, Impacts Lower Limb Joint Work during Walking and Stair Ascent. Journal of functional morphology and kinesiology, 8(4), 145. https://doi.org/10.3390/jfmk8040145

Whittle, M. W. (2007). Gait analysis: an introduction (4th ed.). Butterworth-Heinemann.

Yentes, J. M., Hunt, N., Schmid, K. K., Kaipust, J. P., McGrath, D., & Stergiou, N. (2013). The appropriate use of approximate entropy and sample entropy with short data sets. Annals of biomedical engineering, 41(2), 349–365. https://doi.org/10.1007/s10439-012-0668-3

Yentes, J. M., Denton, W., McCamley, J., Raffalt, P. C., & Schmid, K. K. (2018). Effect of parameter selection on entropy calculation for long walking trials. Gait & posture, 60, 128–134. https://doi.org/10.1016/j.gaitpost.2017.11.023

Yentes, J. M., & Raffalt, P. C. (2021). Entropy Analysis in Gait Research: Methodological Considerations and Recommendations. Annals of biomedical engineering, 49(3), 979–990. https://doi.org/10.1007/s10439-020-02616-8

Zeng, X., Xie, Z., Zhong, G., Chen, Y., Wen, B., Li, Y., Ma, L., Huang, W., Yang, T., & Zhang, Y. (2022). The 6DOF knee kinematics of healthy subjects during sloped walking compared to level walking. Gait & posture, 95, 198–203. https://doi.org/10.1016/j.gaitpost.2022.05.004

Zeni, J. A., Richards, J. G., & Higginson, J. S. (2008). Two simple methods for determining gait events during treadmill and overground walking using kinematic data. Gait & Posture, 27(4), 710–714. https://doi.org/10.1016/j.gaitpost.2007.07.007

Zoffoli, L., Ditroilo, M., Federici, A., & Lucertini, F. (2017). Local stability and kinematic variability in walking and pole walking at different speeds. Gait & posture, 53, 1–4. https://doi.org/10.1016/j.gaitpost.2016.12.017

APPENDIX 1.

Calculation of spatiotemporal parameters		
Parameter	Description	Calculation Method
Speed (m/s)	Walking speed	Converted from km/h to m/s
Left stride time (s)	Average stride time for the left foot	Mean of the differences between consecutive FS_L values, converted to milliseconds
Right stride time (s)	Average stride time for the right foot	Mean of the differences between consecutive FS_R values, converted to milliseconds
Step time (s)	Average step time	Mean of the differences between consecutive step events (FS_L and FS_R combined), converted to milliseconds
Left stride length (m)	Average stride length for the left foot	Left stride time multiplied by speed
Right stride length (m)	Average stride length for the right foot	Right stride time multiplied by speed
Step length (m)	Average step length	Step time multiplied by speed

Cadence (1/min)	Steps per minute	Speed divided by step length, then multiplied by 1000 and 60
Left stance duration (s)	Average stance phase duration for the left foot	Mean of the differences between FO_L and the closest preceding FS_L, converted to milliseconds
Right stance duration (s)	Average stance phase duration for the right foot	Mean of the differences between FO_R and the closest preceding FS_R, converted to milliseconds
Left swing duration (s)	Average swing phase duration for the left foot	Mean of the differences between FS_L and the closest preceding FO_L, converted to milliseconds
Right swing duration (s)	Average swing phase duration for the right foot	Mean of the differences between FS_R and the closest preceding FO_R, converted to milliseconds
Left stance phase (%)	Average proportion of stance phase duration in a gait cycle for the left foot	Mean values of left stance phase duration divided by left stride time
Right stance phase (%)	Average proportion of stance phase duration in a gait cycle for the right foot	Mean values of right stance phase duration divided by right stride time
FS_L: frame numbers where left foot strikes occur FS_R: frame numbers where right foot strikes occur FO_L: frame numbers where left foot offs occur FO_R: frame numbers where right foot offs occur		

APPENDIX 2.

The figures illustrate one participant's joint angles during walking across all inclinations, with forty consecutive strides represented in different colors.

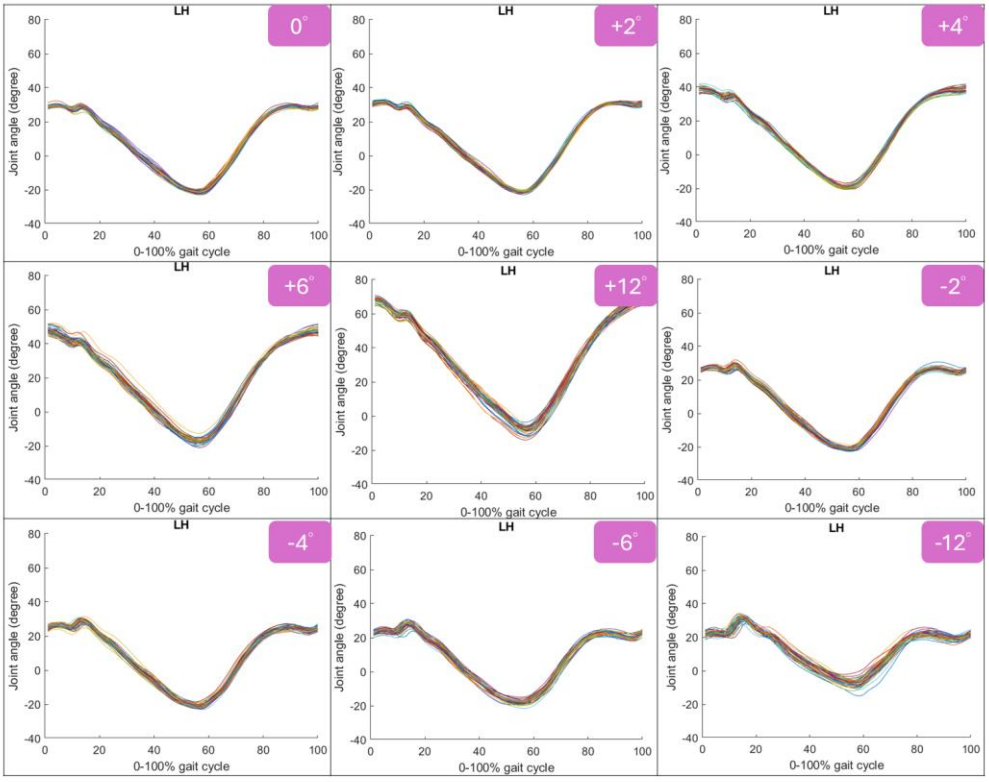

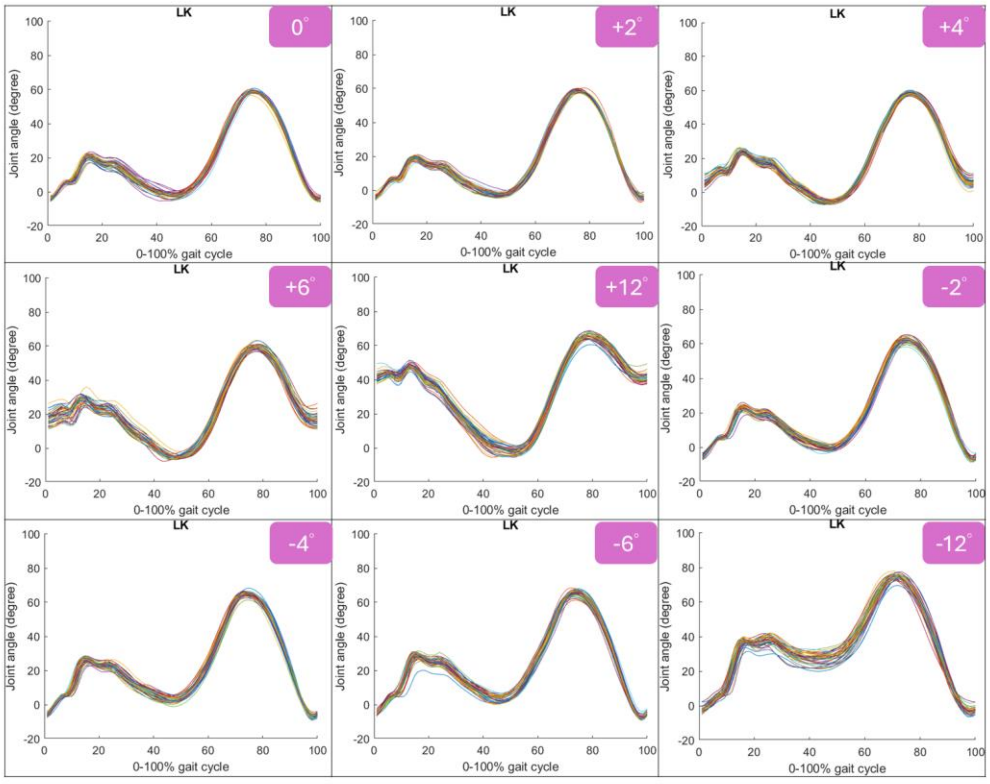

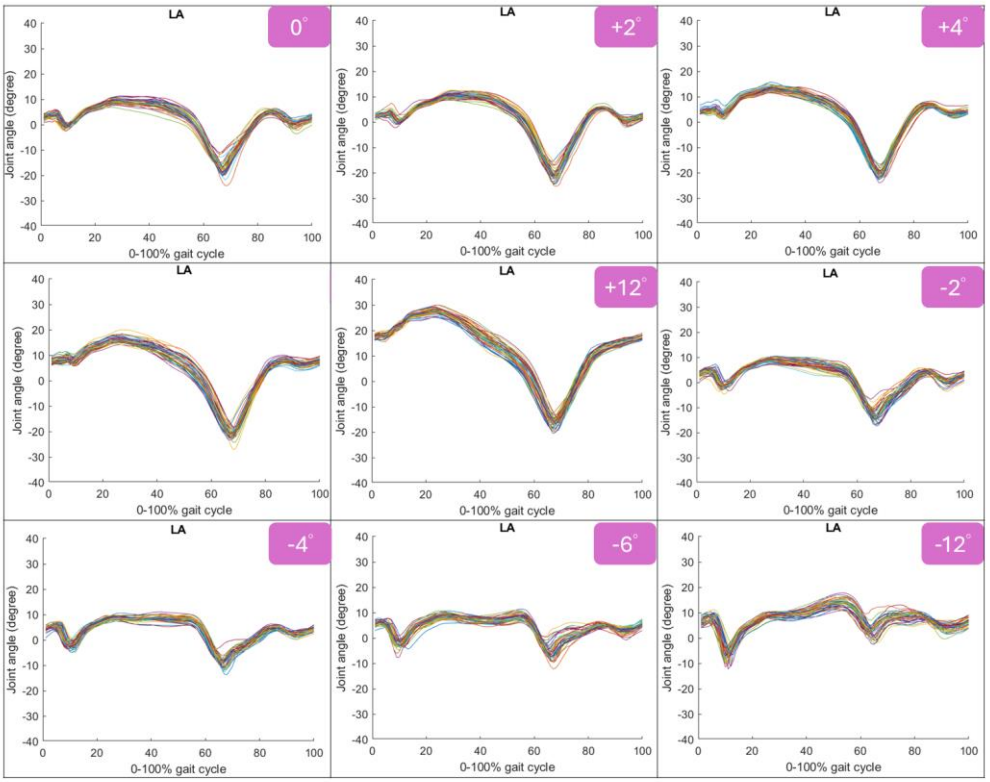
LA
0°
+2°
+4°
+12°
-2°
-4°
-6°
-12°
Joint angle (degree)
0-100% gait cycle

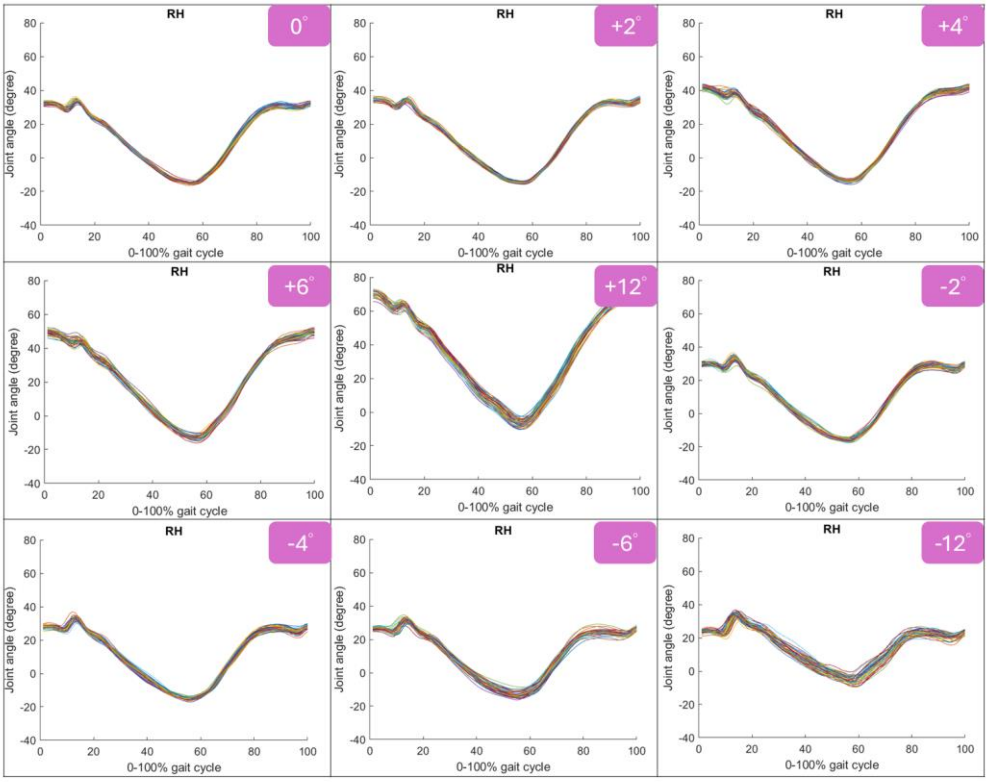
RH
0°
+2°
+4°
+6°
+12°
-2°
-4°
-6°
-12°
Joint angle (degree)
0-100% gait cycle

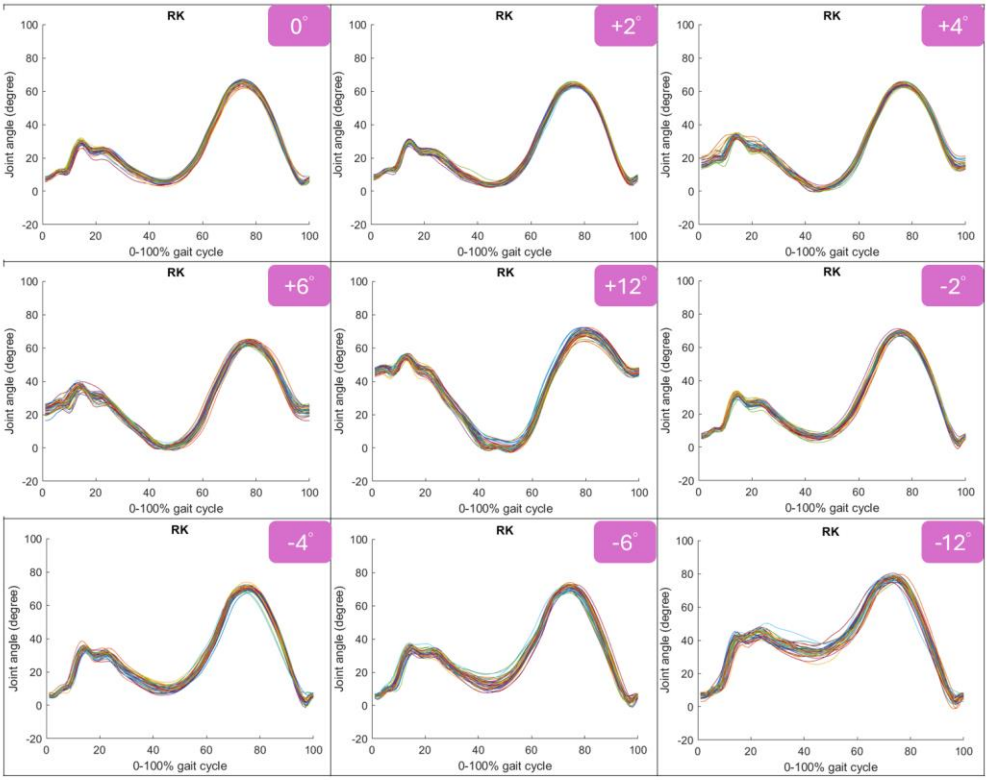
RK
0°
+2°
+4°
+6°
+12°
-2°
-4°
-6°
-12°
Joint angle (degree)
0-100% gait cycle

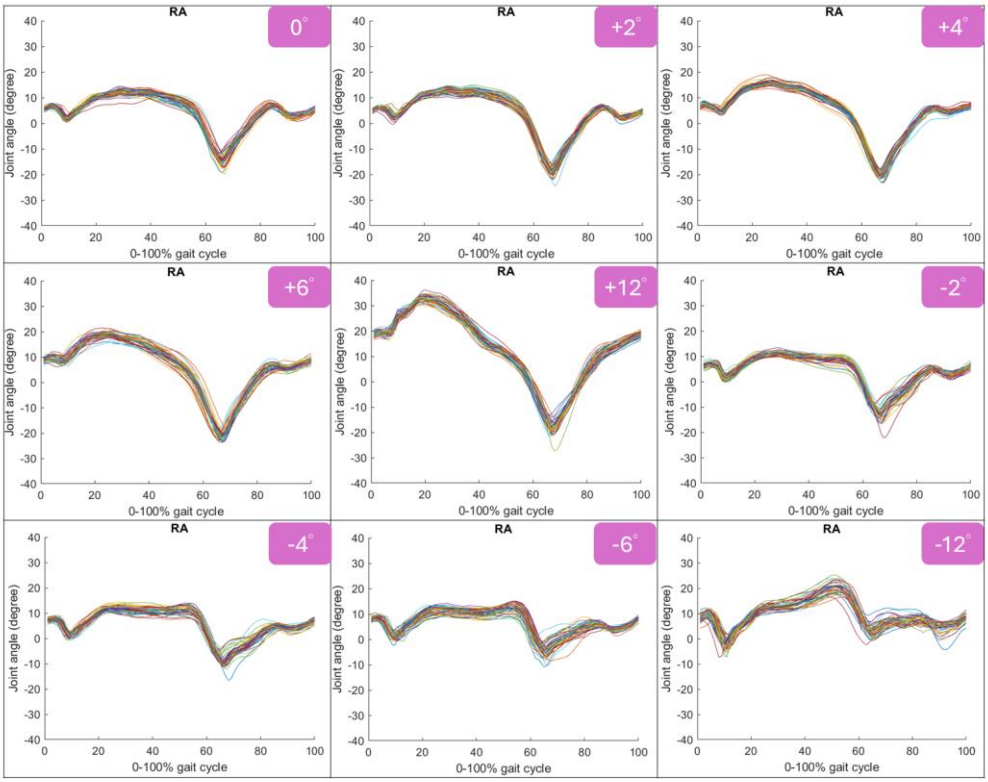
RA
0°
+2°
+4°
+6°
+12°
-2°
-4°
-6°
-12°
Joint angle (degree)
0-100% gait cycle

APPENDIX 3.

The figures present the results of SampEn (m=2) computed with different r values. The x-axis is the value of SampEn (bits), and the y-axis is the r value.

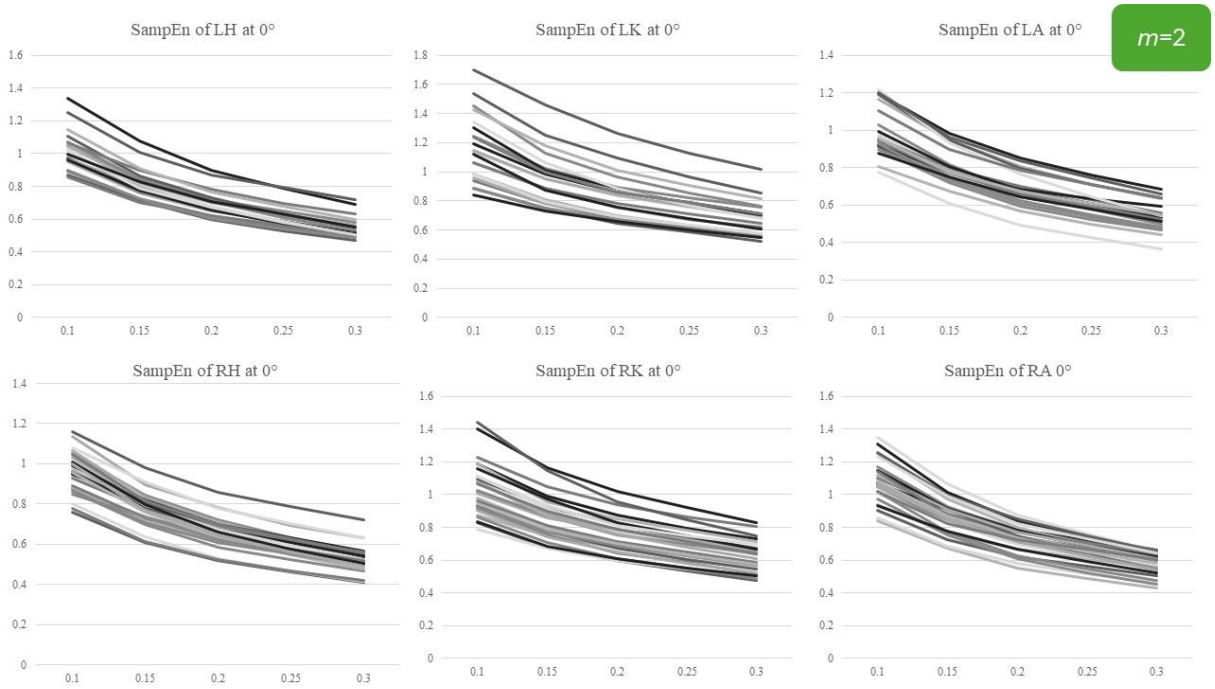

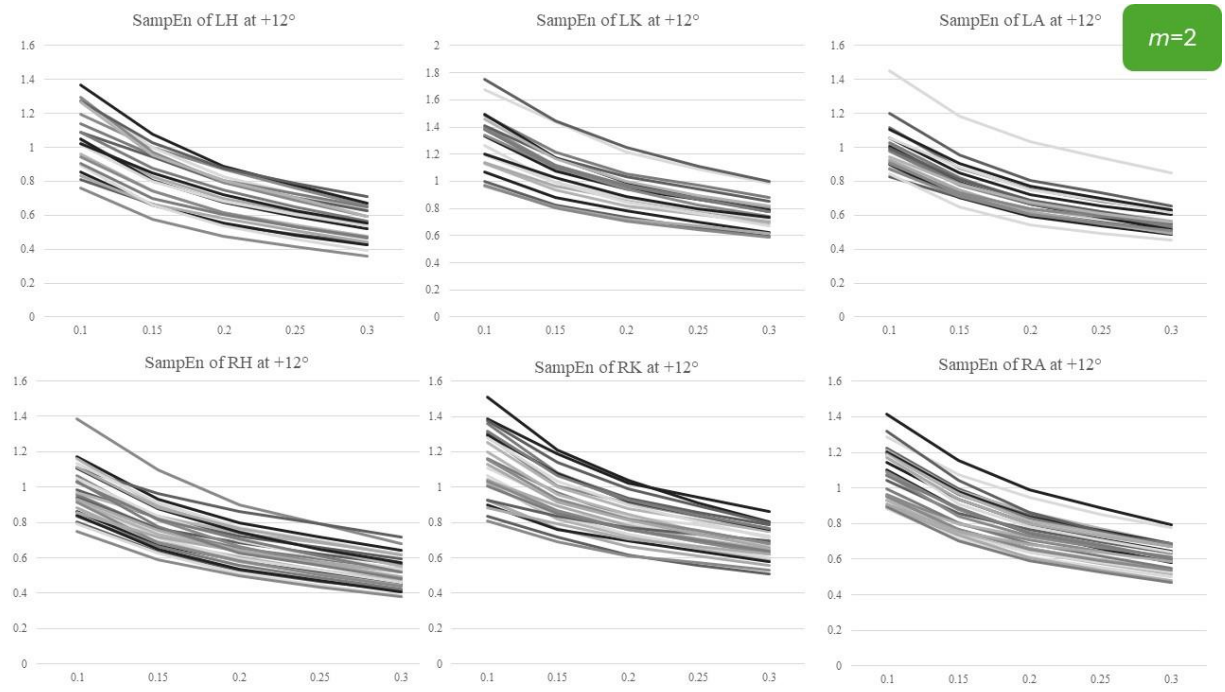

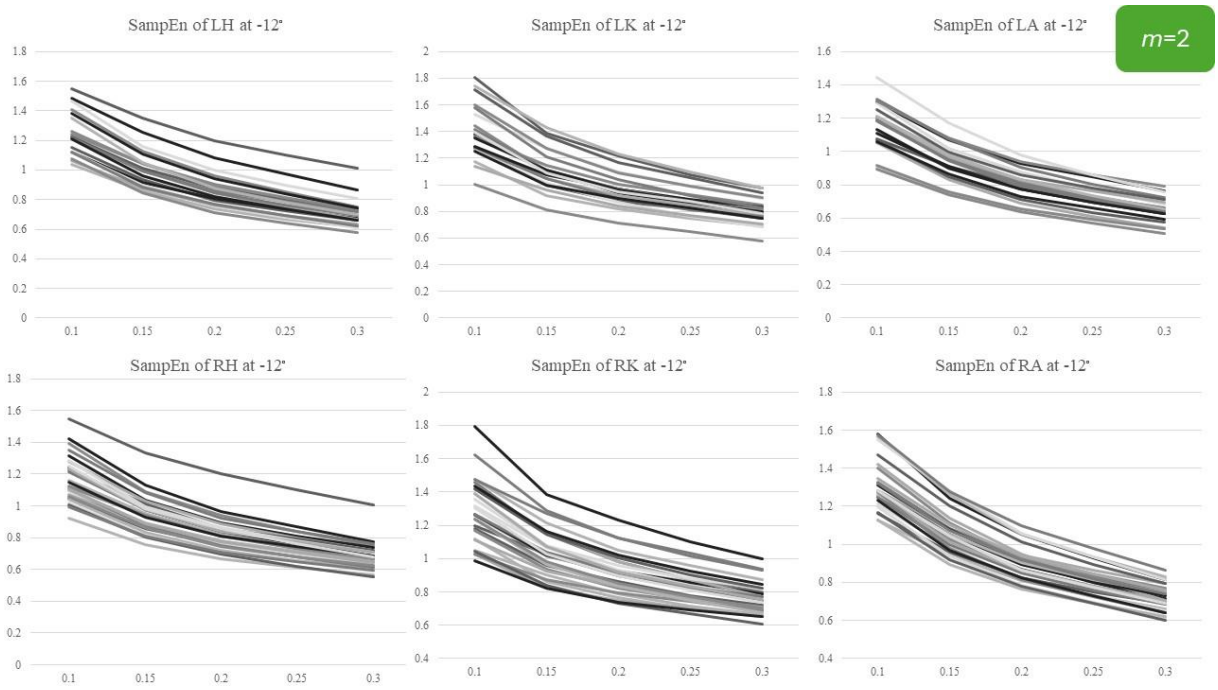
SampEn of LH at -12°
SampEn of LK at -12°
SampEn of LA at -12°
m=2
SampEn of RH at -12°
SampEn of RK at -12°
SampEn of RA at -12°

APPENDIX 4.

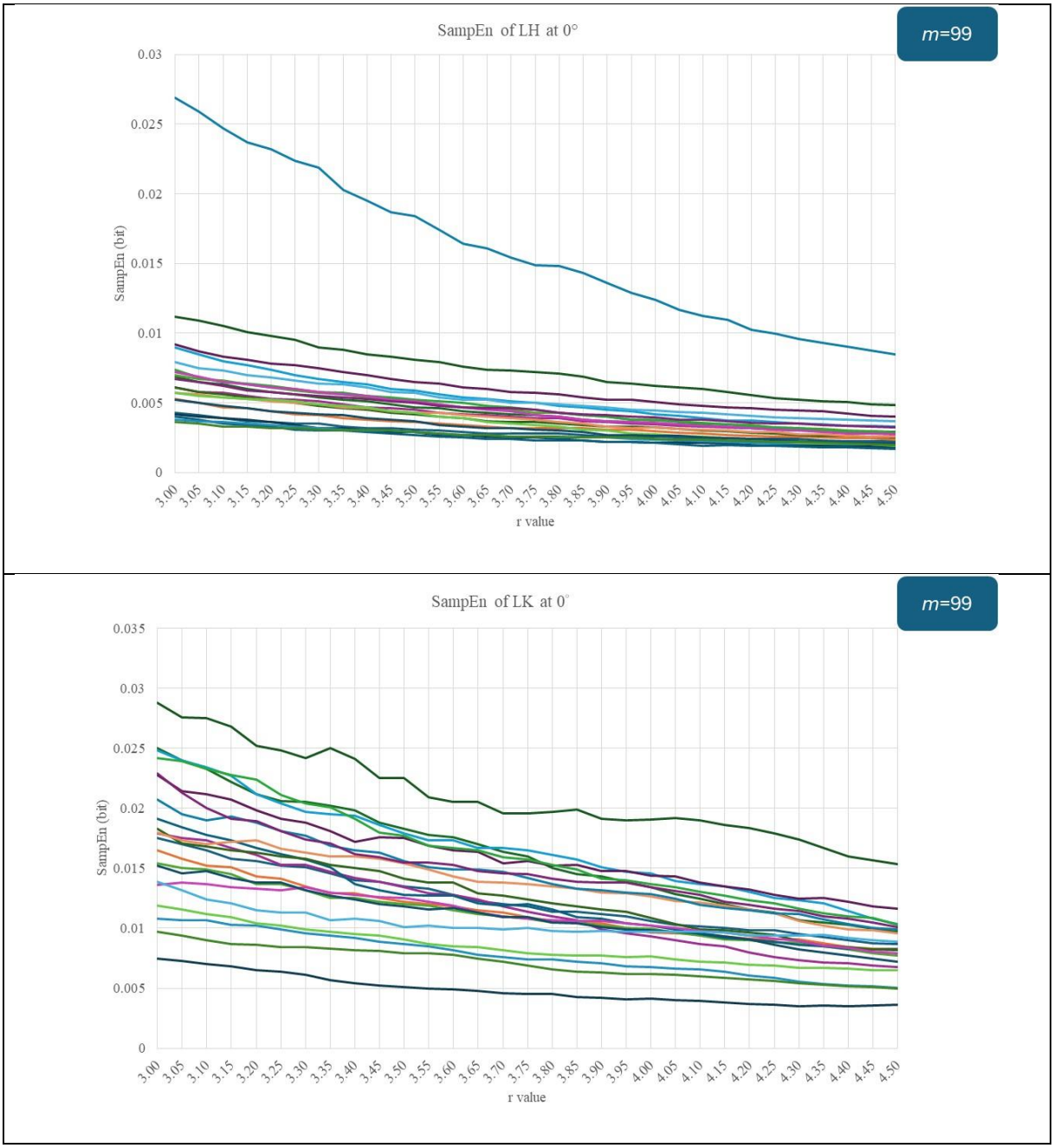
SampEn of LH at 0°
m=99
SampEn (bit)
r value
SampEn of LK at 0°
m=99
SampEn (bit)
r value

m=99

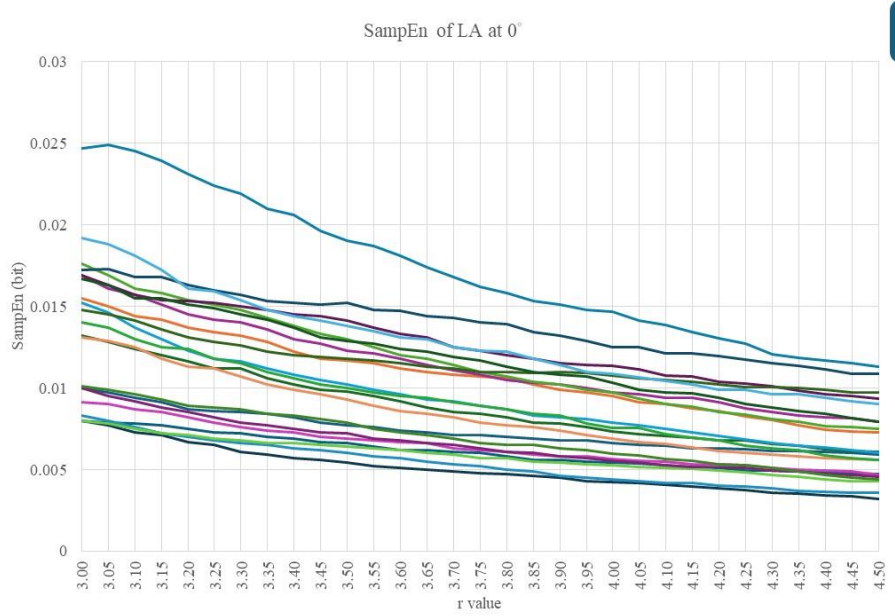
SampEn of LA at 0°
SampEn (bit)
0.03
0.025
0.02
0.015
0.01
0.005
0
3.00 3.05 3.10 3.15 3.20 3.25 3.30 3.35 3.40 3.45 3.50 3.55 3.60 3.65 3.70 3.75 3.80 3.85 3.90 3.95 4.00 4.05 4.10 4.15 4.20 4.25 4.30 4.35 4.40 4.45 4.50
r value

m=99

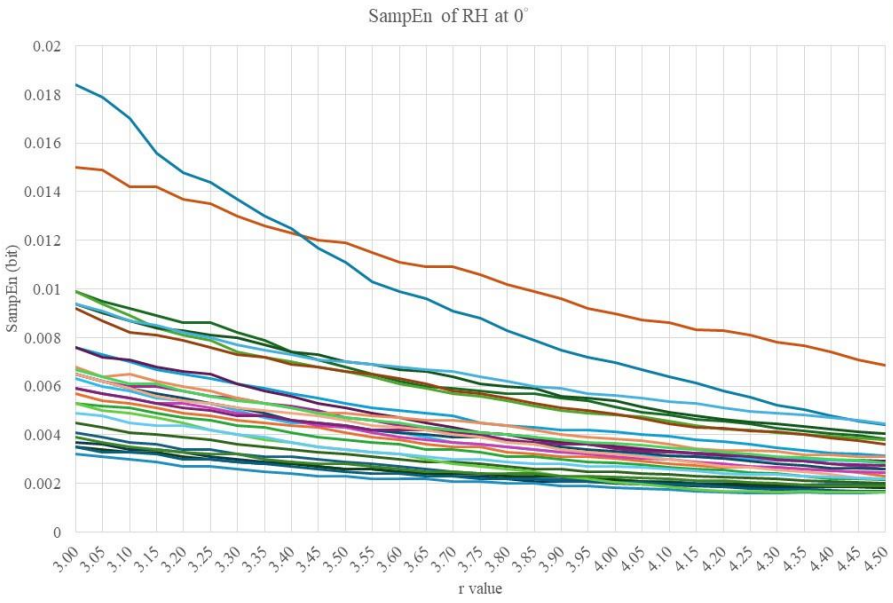
SampEn of RH at 0°
SampEn (bit)
0.02
0.018
0.016
0.014
0.012
0.01
0.008
0.006
0.004
0.002
0
3.00 3.05 3.10 3.15 3.20 3.25 3.30 3.35 3.40 3.45 3.50 3.55 3.60 3.65 3.70 3.75 3.80 3.85 3.90 3.95 4.00 4.05 4.10 4.15 4.20 4.25 4.30 4.35 4.40 4.45 4.50
r value

m=99

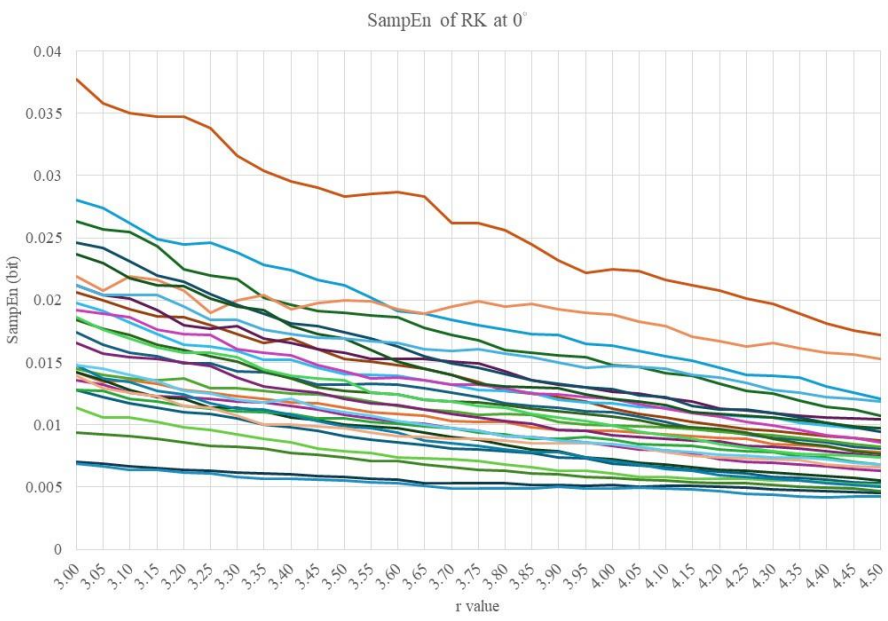
SampEn of RK at 0°
SampEn (bit)
0.04
0.035
0.03
0.025
0.02
0.015
0.01
0.005
0
3.00 3.05 3.10 3.15 3.20 3.25 3.30 3.35 3.40 3.45 3.50 3.55 3.60 3.65 3.70 3.75 3.80 3.85 3.90 3.95 4.00 4.05 4.10 4.15 4.20 4.25 4.30 4.35 4.40 4.45 4.50
r value

m=99

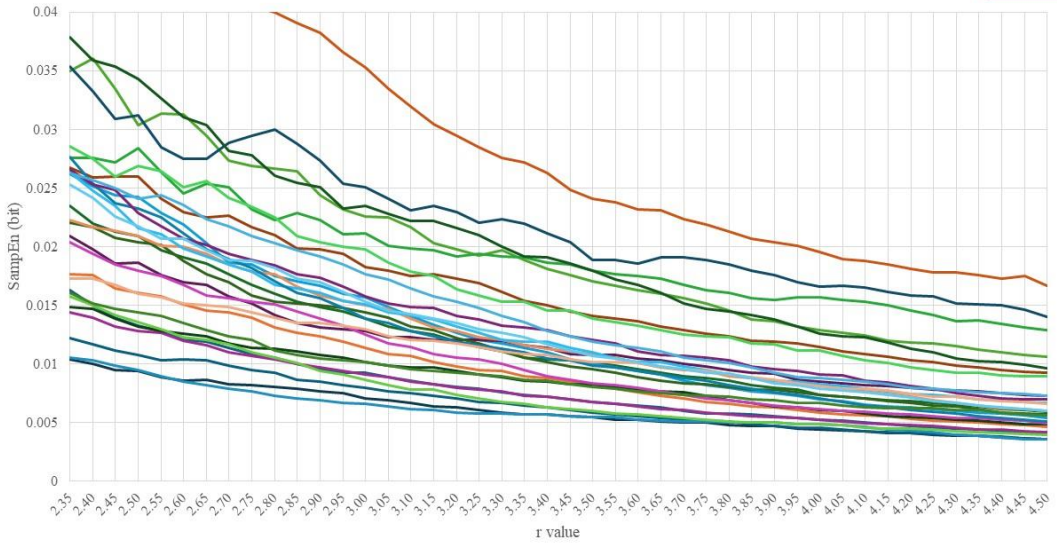
SampEn of RA at 0°
SampEn (bit)
0.04
0.035
0.03
0.025
0.02
0.015
0.01
0.005
0
2.35 2.40 2.45 2.50 2.55 2.60 2.65 2.70 2.75 2.80 2.85 2.90 2.95 3.00 3.05 3.10 3.15 3.20 3.25 3.30 3.35 3.40 3.45 3.50 3.55 3.60 3.65 3.70 3.75 3.80 3.85 3.90 3.95 4.00 4.05 4.10 4.15 4.20 4.25 4.30 4.35 4.40 4.45 4.50
r value


SampEn of LH at +12°
m=99
SampEn (bit)
r value
SampEn of LK at +12°
m=99
SampEn (bit)
r value

m=99

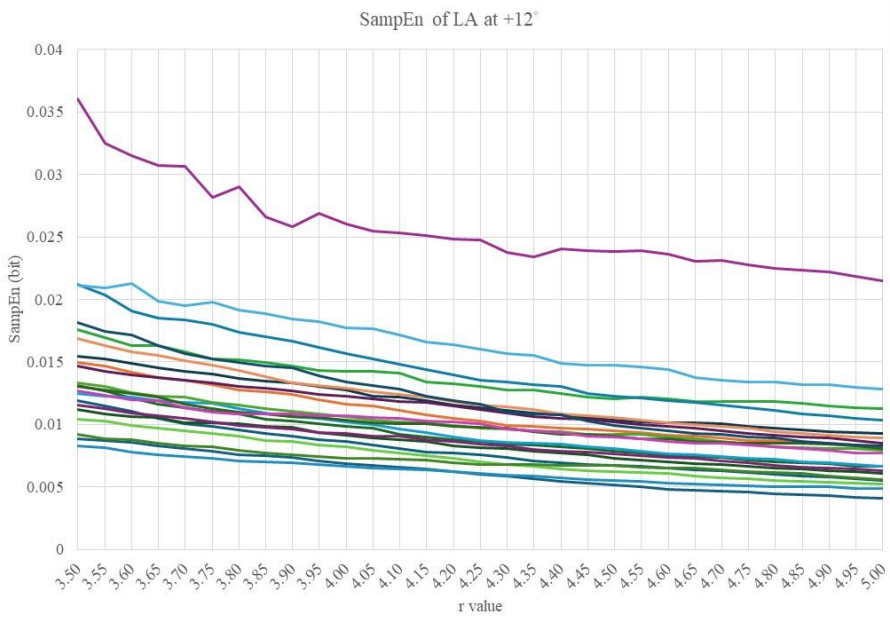
SampEn of LA at +12°
SampEn (bit)
0.04
0.035
0.03
0.025
0.02
0.015
0.01
0.005
0
3.50 3.55 3.60 3.65 3.70 3.75 3.80 3.85 3.90 3.95 4.00 4.05 4.10 4.15 4.20 4.25 4.30 4.35 4.40 4.45 4.50 4.55 4.60 4.65 4.70 4.75 4.80 4.85 4.90 4.95 5.00
r value

m=99

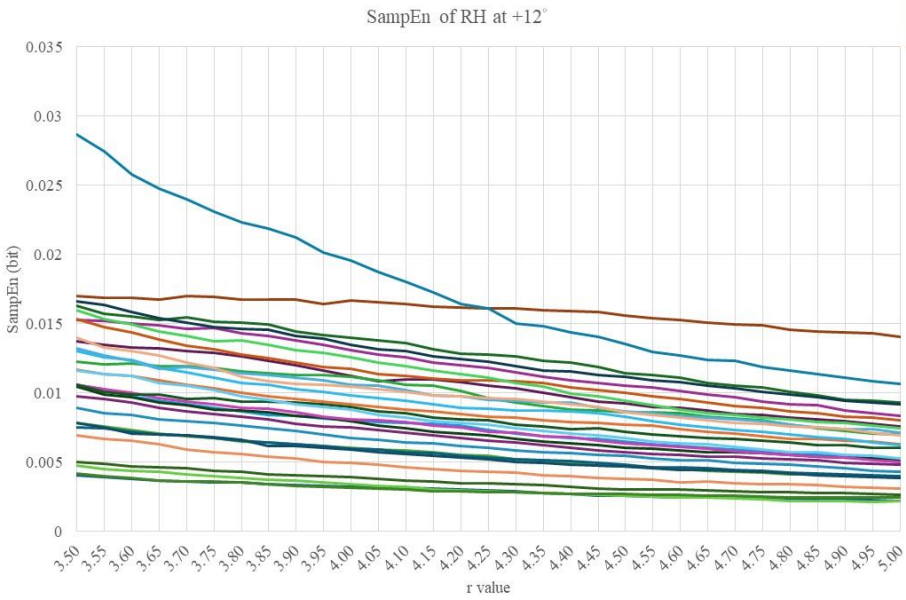
SampEn of RH at +12°
SampEn (bit)
0.035
0.03
0.025
0.02
0.015
0.01
0.005
0
3.50 3.55 3.60 3.65 3.70 3.75 3.80 3.85 3.90 3.95 4.00 4.05 4.10 4.15 4.20 4.25 4.30 4.35 4.40 4.45 4.50 4.55 4.60 4.65 4.70 4.75 4.80 4.85 4.90 4.95 5.00
r value

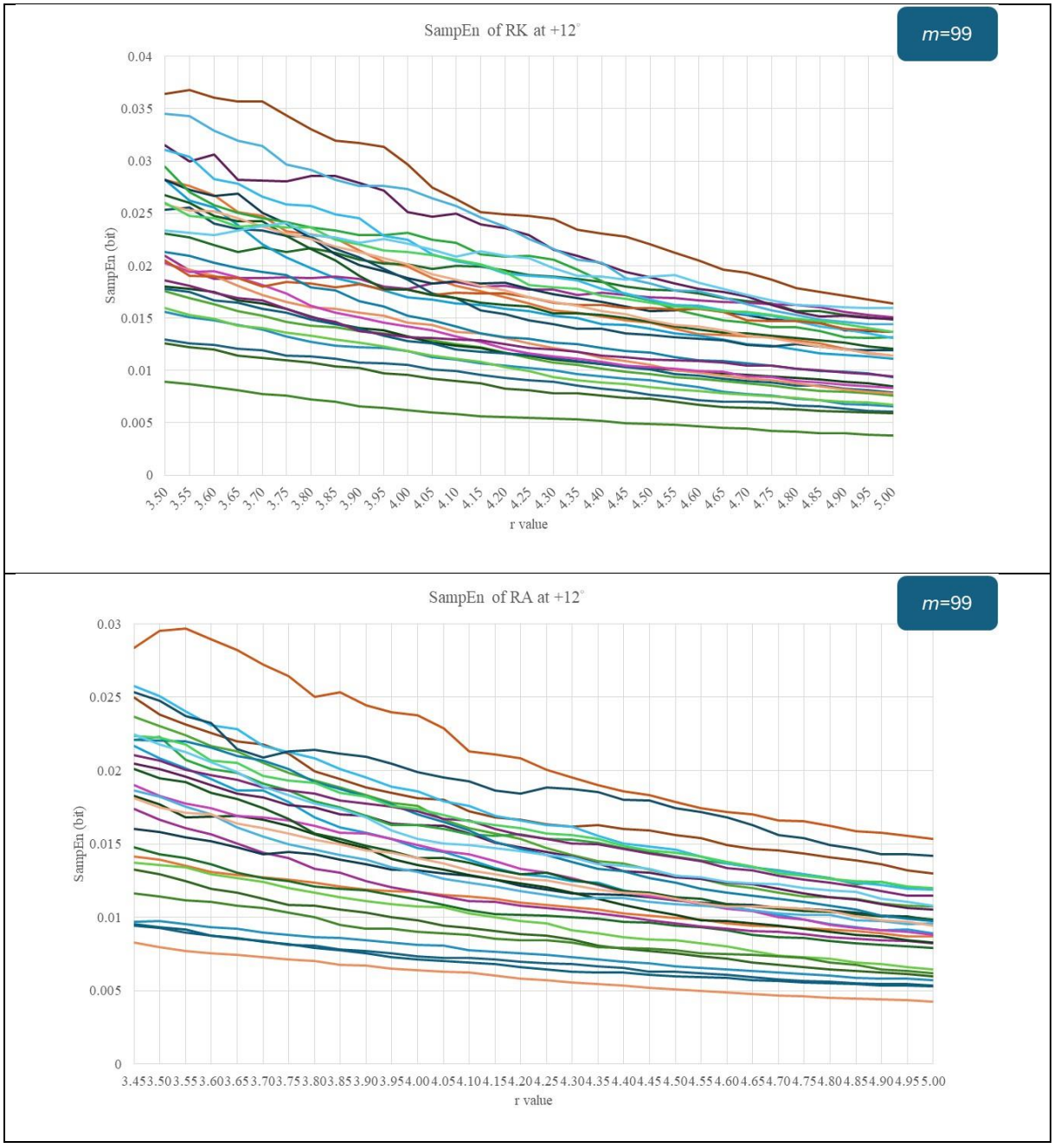
SampEn of RK at +12°
m=99
SampEn (bit)
r value
SampEn of RA at +12°
m=99
SampEn (bit)
r value

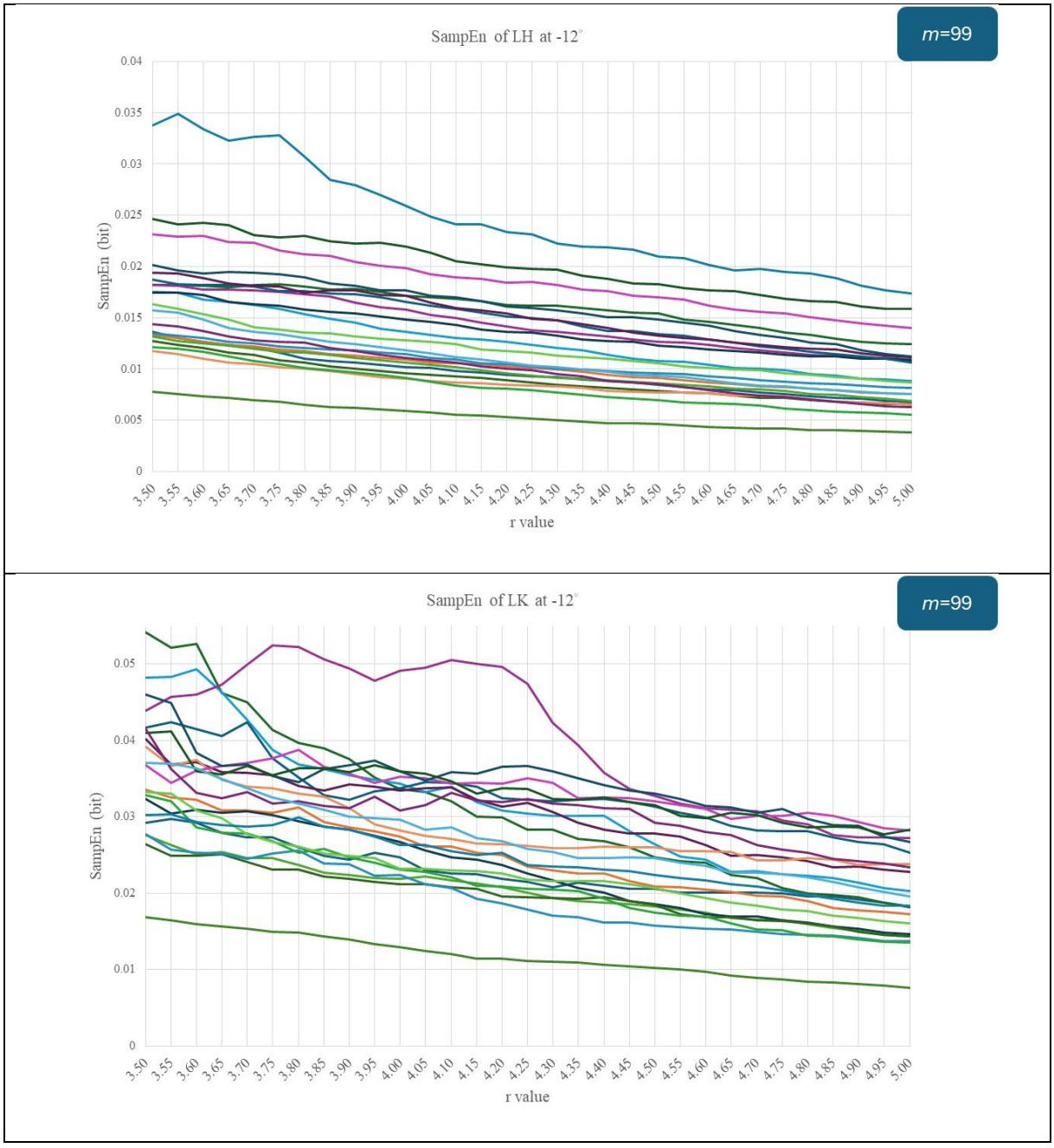
SampEn of LH at -12°
m=99
SampEn (bit)
r value
SampEn of LK at -12°
m=99
SampEn (bit)
r value

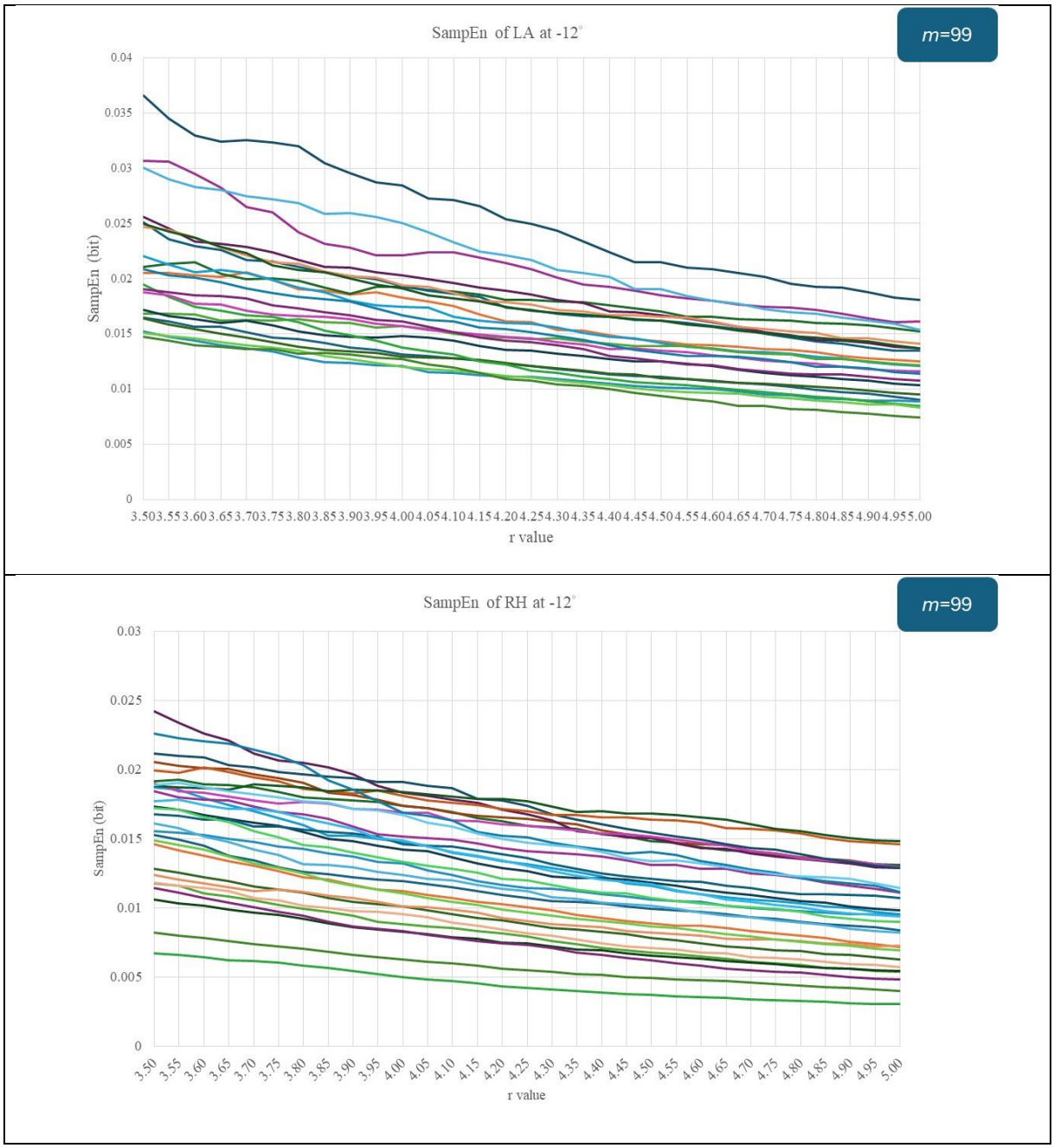
SampEn of LA at -12°
m=99
SampEn (bit)
0.04
0.035
0.03
0.025
0.02
0.015
0.01
0.005
0
3.50 3.55 3.60 3.65 3.70 3.75 3.80 3.85 3.90 3.95 4.00 4.05 4.10 4.15 4.20 4.25 4.30 4.35 4.40 4.45 4.50 4.55 4.60 4.65 4.70 4.75 4.80 4.85 4.90 4.95 5.00
r value
SampEn of RH at -12°
m=99
SampEn (bit)
0.03
0.025
0.02
0.015
0.01
0.005
0
3.50 3.55 3.60 3.65 3.70 3.75 3.80 3.85 3.90 3.95 4.00 4.05 4.10 4.15 4.20 4.25 4.30 4.35 4.40 4.45 4.50 4.55 4.60 4.65 4.70 4.75 4.80 4.85 4.90 4.95 5.00
r value


m=99
SampEn of RK at -12°
SampEn (bit)
0.08
0.07
0.06
0.05
0.04
0.03
0.02
0.01
0
3.50 3.55 3.60 3.65 3.70 3.75 3.80 3.85 3.90 3.95 4.00 4.05 4.10 4.15 4.20 4.25 4.30 4.35 4.40 4.45 4.50 4.55 4.60 4.65 4.70 4.75 4.80 4.85 4.90 4.95 5.00
r value
m=99
SampEn of RA at -12°
SampEn (bit)
0.05
0.04
0.03
0.02
0.01
0
3.50 3.55 3.60 3.65 3.70 3.75 3.80 3.85 3.90 3.95 4.00 4.05 4.10 4.15 4.20 4.25 4.30 4.35 4.40 4.45 4.50 4.55 4.60 4.65 4.70 4.75 4.80 4.85 4.90 4.95 5.00
r value